AN INVESTIGATION OF A REACTOR SYSTEM FOR TWO SECOND ORDER CONSECUTIVE HOMOGENEOUS LIQUID REACTIONS

A Dissertation

Presented for the Degree

of

Master of Science in Chemical Engineering

by

John Robert Brigg B.Sc. (Chem. Eng.) (Rand)

This work was carried out in the Department of Chemical Engineering under the supervision of:

Professor D. Glasser, B.Sc. (A. & I.C.) (Cape Town), Ph.D. (Lond), D.I.C.

and

Dr. C.B. Schlesinger, M.Sc. (Eng.) (Rand), Ph.D. (Lond), D.I.C.

UNIVERSITY OF THE WITWATERSRAND, JOHANNESBURG

DECEMBER, 1971.

DECLARATION

The work described in this dissertation was carried out in the Department of Chemical Engineering in the University of the Witwatersrand and is the original and independent work of the author except where specifically acknowledged in the text.

No part of this dissertation has previously been submitted in candidature for a degree in the University of the Witwatersrand, or is being submitted to any other university.

J. R. Briggs.

December, 1971.

ACKNOWLEDGMENTS

The author wishes to tend his grateful thanks to the following:-

Professor Glasser and Dr. Schlesinger for their keen interest and guidance during the course of this work.

Mr. Newey and Mr. Kauril for their considerable help in construction and maintenance of experimental apparatus.

INDEX TO CHAPTERS

APPENDICES

CHAPTER 1

1.1 INTRODUCTION

As Levenspiel (1962) has said, "The design of chemical reactors is probably the one area of interest in engineering that is unique to chemical engineering, and it is probably this function more than anything else which justifies the existence of chemical engineering as a distinct branch of engineering."

In the chemical engineering design of reactors, knowledge is required in the fields of chemical kinetics, economics, mathematics, thermodynamics and heat, mass and momentum transfer.

There are four main stages in the design of chemical reactors:-

1.1.1 Choice of Reaction and Determination of Reaction Kinetics

The decision to build a chemical plant, choice of reaction, raw materials and products may well be outside the scope of the reactor design engineer. Generally, the reactor designer will also not be required to obtain kinetic data for the reactor. These, together with the required production rates will be made available to him at the outset of the design. (Denbigh, 1965). His task, therefore, will be to use the information supplied to design a reactor which will require minimum acceptable capital expenditure and operate as economically as possible.

1.1.2 Evaluation of Possible Reactor Types

It is necessary to obtain a mathematical model for each possible type of reactor. The most accurate model will, of course, be that obtained by solving differential heat, mass and momentum balances in the reactor. The number of variables in industrial reactors is apt to be large, however, and the resulting differential equations may be

complex. The engineer will thus be forced to make simplifying assumptions in order to solve them. Boundary conditions for the equations will also have to be decided. Unfortunately, each different assumption made, and each set of boundary conditions chosen is liable to lead to a different mathematical model for the reactor, and the designer will have to decide which of these best describes the behaviour of the real reactor.

In many cases pilot plant studies can be used to evaluate the models and choose the most accurate. Without such studies, however, choice of a mathematical model is extremely difficult.

1.1.3 Economic Model of Reactor (Profit Function)

Economic information relating reactor variables to plant profit can be incorporated in the mathematical model obtained in 1.1.2 to give an economic model for the reactor. The economic model will thus relate the reactor variables to plant profitability, and will provide a profit function which can be optimised by suitable choice of reactor variables. This economic model must include interaction between the reactor and other items of equipment on the plant.

1.1.4 Design of Optimum Reactor

Combining the mathematical and economic models above, the optimum operating conditions and reactor design can be obtained for each reactor type in 1.1.2. The optimum reactor can now be chosen.

This completes the design engineer's task.

1.2 SCOPE OF THIS INVESTIGATION

An attempt has been made in this thesis to approach the design of a reactor in as realistic a manner as possible, and to study and elucidate some of the problems encountered. The design of a laboratory scale reactor was accordingly carried out as outlined

in 1.1, although a complete economic model as in 1.1.3 could not be obtained and a simplified profit function was assumed. The reactor was then constructed and the various mathematical models tested.

CHAPTER 2

2.1 CHOICE OF REACTION SYSTEM

As stated in the introduction, the reaction system and reaction kinetics will usually be supplied to the design engineer. For this work, however, a reaction system had to be chosen which would best illustrate certain of the problems encountered in reactor design.

A reaction system was required on which some form of optimisation could be carried out for one of the reacting species. A simple example would be consecutive irreversible first order reactions of the type A→B→C, with the possibility of optimising B concentration.

In order to show up inaccuracies in the various mathematical models, however, non-linear kinetics would be better than linear, (Levenspiel and Bischoff, 1959), so a set of consecutive reactions with non-linear kinetics was sought.

In order to minimise experimental difficulties involved in obtaining diffusivities, analysing reaction mixtures, calibrating flowmeters and carrying out temperature control policies, it was decided that a homogeneous reaction in liquid medium was preferable.

It was felt that stagewise saponification reactions of the esters of dibasic acids or dihydric alcohols might be suitable, and accordingly a literature survey was carried out to discover reaction velocity constants for these reaction systems.

Meyer, (1909), studied the kinetics and obtained the rate constants for both the acidic and basic saponification of a wide variety of dibasic and di- and trihydric esters. Of these reactions, the basic saponification rate constants appeared to be of acceptable

order. Two practical difficulties arose at this point, however, the first being the problem of obtaining raw materials for the reaction in large quantities, and the second, the experimental difficulty involved in analysing the reaction mixtures.

Eventually, the stagewise saponification of ethylene glycol diacetate was chosen, since ethylene glycol diacetate, 98,9% purity, could be obtained from the Dow Chemical Company, and the reaction mixture could be analysed by stardard wet chemistry techniques.

2.2 REACTION MECHANISM

It was Meyer, (1907, 1909), who first realised that the alkaline saponification reactions of the esters of dibasic acids and dihydric alcohols were second order and consecutive. Different mechanisms had been proposed for the reactions by Geitel, (1897, 1898), Knoblauch (1898), Ostwald (1902), and Kremann, (1905).

None of the mechanisms assumed by these workers yielded reproducible values of reaction velocity constants for different inlet concentrations, however, and all were abandoned. Kremann, (1905), studied both ethylene glycol diacetate and monoacetate alkaline saponifications, and assumed that each reaction was bimolecular but did not assume that the reactions were consecutive. He was thus able to get reproducible values of the rate constants for the monoacetate saponification, but not for the diacetate.

Finally, Meyer, (1907, 1909), studied the individual steps in the saponification reactions, first in acid and then in alkaline media. He worked with a wide variety of esters, using those of dibasic acids and di- and trihydric alcohols. He proposed that the saponifications were consecutive and that each step was bimolecular. Since he was able to obtain reproducible values of the rate constants, this mechanism has been accepted. For the alkaline saponifi-

cation of ethylene glycol diacetate, the reaction scheme is as follows:-

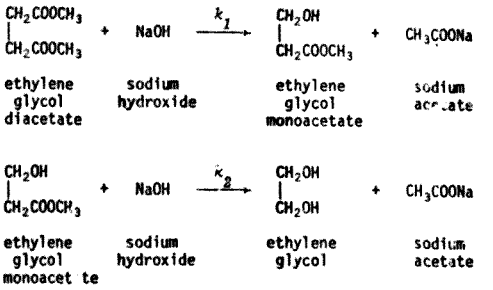

k_1 and k_2 are the rate constants of reactions I and II respectively.

2.3 REACTION KINETICS

2.3.1 Previous work

Meyer, (1909), did two sets of runs in a batch reactor to obtain the reaction rate constants k_1 and k_2 for reactions I and II.

In the first set, pure monoacetate was reacted with caustic soda. This meant that only reaction II was proceeding in the solution and the reaction velocity constant, k_2, could be obtained from a knowledge of the inlet concentrations and by measuring the rate of change of caustic soda concentration with time.

In the second set of runs, pure diacetate was used, which meant that reactions I and II took place simultaneously in the solution. In order to solve the resulting rate equations for the reaction rate constant, k_1, Meyer was forced to assume a relationship between k_1 and k_2. Since he had found the ratio in acid medium to be $k_1:k_2::2:1$, Meyer assumed that the ratio for alkaline saponification would be the same. Having made this assumption, he was able

to solve for k_1, in the same fashion as for k_2, i.e. by a knowledge of initial diacetate and caustic concentrations, and the rate of change of caustic concentration with time, (see Appen. vii).

Meyer's results are tabulated below:-

TABLE 2.1

Initial Diacetate conc. (M)	Initial Monoacetate conc. (M)	Initial Caustic conc.(M)	Temp. °C.	k_1 litre/gm. mole min.	k_2 litre/gm. mole min.	$2k_2$
0	0,01268	0,01	18	-	8,734	17,468
0	0,04906	0,05	18	-	7,444	14,888
0	0,01268	0,01	25	-	15,905	31,810
0	0,01932	0,02	25	-	16,719	33,438
0,02000	0	0,02	18	15,334	-	-
0,01000	0	0,01	18	15,040	-	-
0,01174	0	0,01	25	32,456	-	-
0,05286	0	0,05	25	32,862	-	-

Note: Meyer's concentrations are given in cm^3 of 0,01 N HCl used to titrate 25 cm^3 of alkaline sample. Hence all concentrations in his tables must be multiplied by 0,01/25 to transform them to gm.moles/litre (M).

The reproducible values obtained for k_2 show that the reaction II rate data are fitted by a bimolecular model. By writing the Arrhenius relationship in the form

$$\log k_2 = a + bT$$

and solving for a and b from his results, Meyer was able to extrapolate his k_2 values to 0°C and 19,8°C and compare them with Kremann's (1905) values of k_2 at these temperatures. The values are given below in litre/gm.mole min.

TABLE 2.2

Temp. °C	Kremann k_2	Meyer k_2
0	2,5	1,33
19,9	12,5	9,69

Meyer felt that the agreement between these results was satisfactory.

Since the k_1 values do not differ greatly from each other, and since they are all roughly twice the k_2 values at the same temperature, Meyer concluded that reaction I is also bimolecular and that $k_1 = 2k_2$

There are several possible sources of inaccuracies in Meyer's work. Firstly it is difficult to determine the accuracy of the approximation that $k_1 = 2k_2$ from Meyer's results. Secondly, Meyer does not report the purity of his raw materials, and if they were not 100% pure, this would, of course, produce errors in his calculated k values. Thirdly, Meyer pipetted samples out of his batch reactor and ran them into acid solution to quench the reaction. No mention is made of the time taken to quench the samples, and if this was great, the reactor concentrations would be in error. Lastly, the acid saponification reactions will take place slowly in the quenched solution, and these produce acetic acid (see 8.4), hence backtitration must be done soon after quenching or else errors in concentration will be introduced. Meyer makes no mention of taking this precaution.

Since caustic soda concentration in the reaction mixture is easiest to follow, it was decided that this would be measured during the kinetic experiments, and a regression technique (see 2.3.4) used to obtain the best k_1 and k_2. (Note: Meyer (1909) in Tables 1-8 (pages

268-271) gives his concentration of NaOH vs time data, so the regression technique was also applied to these.)

2.3.2 Batch Reactor

Initially it was decided that a batch reactor would be used to check Meyer's results for diacetate and monoacetate. The reactants would be mixed in the reactor at time $t=0$, and samples of reaction mixture would be withdrawn from time to time and quenched in hydrochloric acid solution. This solution could subsequently be backtitrated with sodium hydroxide, and the original caustic soda concentration in the reactor thus obtained.

In order to study the possible catalytic effects of materials present in the tubular reactor which was to be used for the main runs, these substances were included in the batch reactor used for the diacetate runs. Thus the diacetate batch reactor wall and floor were constructed of PVC and perspex respectively, since the main reactor was made of perspex, and the reactor system piping was PVC. A stainless steel stirrer was used in the batch reactor, since retaining screens in the main reactor as well as the outlet quench stirrer were made of this material. The stirrer speed for all batch runs was 200 r.p.m. The diacetate reactor was also filled with the same glass beads as those used in the main reactor, these being poured into the reactor with the reactants at the start of the reaction. Diacetate used for these runs was supplied by the Dow Chemical Company and was 98,9% pure, the main impurity being monoacetate. Samples were withdrawn from the diacetate reactor through a wide bore glass tap let into the bottom. The values of rate constants obtained with this reactor show, by their close agreement with Meyer's values, that the above materials had no catalytic effects.

For the monoacetate runs, the reactor used was a simple

glass beaker, and samples were withdrawn with a polythene scoop which held 20 cm^3 of reaction mixture. Unfortunately, only 5/% pure technical grade monoacetate could be obtained from British Drug Houses for these runs.

All samples were stored under high purity nitrogen, in glass beakers fitted with rubber stoppers wrapped in aluminium foil. The titration procedures used were the same as those for the main runs (see Appendix vi - section 1.)

In the reactor optimisation section, 4.3, it was decided that the main runs would be carried out isothermally. It was thus necessary to choose the inlet concentrations for the reactor low enough to limit the temperature rise during reaction to 1°C. On the other hand, the inlet concentration could not be made too low, or the concentration measurements would have become inaccurate.

In order to ensure that the reaction could go to completion, the diacetate and caustic soda inlet concentrations were maintained roughly in the stoichiometric ratio of 1:2. The same ratio was used for the monoacetate runs.

From the runs in the batch reactor, the upper limit of diacetate inlet concentration was found to be 0,1 gm mole/litre, and this could not even be used for the runs at 25°C, because it led to a temperature rise of 2,3°C during reaction.

It was also found that measurement of diacetate concentrations of lower than 0,005 gm.mole/litre led to errors of greater than the 1% specified for this work (see 8.1). The lower limit of diacetate concentration was thus set at 0,005 gm.mole/litre.

The concentrations and temperatures used in the batch runs are given in Table 2.3.

All batch runs were carried out in a constant temperature

room in which the temperature could be thermostatically controlled to within 1°C.

There were several sources of error in the batch experiments. With the highest inlet concentration used, the diacetate reached 50% conversion in 8 seconds, where percentage conversion is defined by:-

$$\frac{(\text{concentration at time } 0 - \text{concentration at time } t)\ 100}{(\text{concentration at time } 0)}$$

The sample time for the diacetate reactor was of the order of 2 seconds, which made the exact quench time very difficult to ascertain for the initial part of the concentration-time curve. The polythene scoop used for the monoacetate runs reduced the quench time to under 0,5 seconds, but led to splashing of the quench solution. For both diacetate and monoacetate runs the concentration of caustic soda towards the end of the run was much lower than at the beginning, and the measurement is consequently less accurate.

In order to reduce acid saponification to a minimum, the quenched solutions were analysed as soon as possible, but since samples were taken for batch residence times of up to 16 minutes, the initial samples had consequently to stand for this length of time before they could be analysed.

2.3.3 Plug Reactor

The difficulties encountered in the batch reactor can all be overcome in a plug reactor system in which the outlet stream is neutralised as soon as it leaves the reactor. The main experimental runs were done in this type of reactor, and the quench and sampling systems are discussed in 5.2.5. With this reactor, outlet caustic concentrations for residence times of from 27 to 116 seconds could be measured very accurately.

The only difficulty in using this type of flow reactor for kinetic measurements is in proving that one does indeed have a plug

flow reactor, and not one which obeys some other model. As will be seen from Chapter 9, the three different models assumed for the reactor all give identical results for different inlet concentrations. Hence, since the plug flow model is the easiest to solve, this can be used to obtain rate constants from measurements taken on the flow reactor.

Two sets of runs were thus done on the plug reactor, neutralising the reactor outlet stream accurately and measuring the outlet caustic concentration. The inlet concentrations and temperatures used for all the batch and flow reactor kinetic experiments, as well as those for Meyer's experiments are given below in Table 2.3. The complete set of kinetic data is given in Appendix x.

2.3.4 Method used for obtaining Rate Constants from Experimental Data

From Table 2.3, it will be seen that the kinetic data cover a range of temperatures. It was thus decided that all the data would be combined and that the reaction rate constants would be obtained as functions of temperature.

From the Arrhenius relationship, we have for each rate constant

$$k = k_{\infty} exp(-E/RT) \qquad 2.1$$

where

k = rate constant (litre/gm.mole min)

k_{∞} = frequency factor (litre/gm.mole min)

E = activation energy (kcal/gm.mole)

R = gas constant (kcal/gm.mole °K)

T = temperature of reaction mixture (°K)

It is difficult to obtain the parameters E and k_{∞} directly because the rate of reaction is far more sensitive to small changes in E than to small changes in k_{∞}. This in turn makes any method of

TABLE 2.3

Temp. °C	NaOH inlet conc.(M)*	Diacetate inlet conc.(M)*	Monoacetate inlet conc.(M)*	Data obtained from
18	0,01	0	0,01268	Meyer
18	0,05	0	0,04906	"
18	0,02	0,02000	0	"
18	0,01	0,01000	0	"
25	0,01	0	0,01268	"
25	0,02	0	0,01932	"
25	0,01	0,01174	0	"
25	0,05	0,05286	0	"
25,0	0,1012	0,04910	0	Diacetate batch
25,0	0,09884	0,05029	0	"
25,0	0,01073	0,004739	0	"
25,0	0,01064	0,004781	0	"
21,5	0,2361	0,0955	0	"
21,5	0,2429	0,09245	0	"
21,5	0,1044	0,04756	0	"
21,5	0,1067	0,04638	0	"
21,5	0,01036	0,005076	0	"
21,5	0,01030	0,005104	0	"
17,0	0,2273	0,09900	0	"
17,0	0,2295	0,09802	0	"
17,0	0,1037	0,04776	0	"
17,0	0,1014	0,04891	0	"
17,0	0,01107	0,004548	0	"
17,0	0,01119	0,004498	0	"
24,0	0,04733	0,01360	0,02972	Monoacetate batch
24,0	0,04982	0,01278	0,02872	"
24,0	0,05473	0,01161	0,02502	"
24,0	0,05425	0,01173	0,02529	"
25,0	0,1188	0,05367	0,002789	Flug Reactor
21,7	0,1195	0,04772	0,002050	"

*(M) = gm.moles/litre.

searching for E and k_∞ very sensitive to small changes in E, and insensitive to changes in k_∞. If the following transformation is made, however,

$$K_\infty = \ln k_\infty \qquad 2.2$$

equation 2.1 becomes:-

$$k = \exp(K_\infty - E/RT) \qquad 2.3$$

K_∞ and E/RT are now of the same order, and have roughly the same effect on the rate constant. They can thus be obtained without difficulty.

The regression technique of King (1967) was used to obtain the values of the above parameters which gave the least sum of squared errors fit between the experimental caustic concentrations and those predicted by the batch and plug flow reactor models.

As can be seen from Table 2.3, there was a spread in the experimental inlet concentrations. It was thus necessary to use a normalised sum of squared errors to prevent the high concentration runs from being weighted disproportionately. The sum of squared errors used was thus:-

$$\text{Sum} = \sum_{\text{expts.}} \frac{(\text{Predicted NaOH conc.} - \text{Experimental NaOH conc.})^2}{(\text{Experimental NaOH conc.})^2}$$

The results of this regression are given below:-

TABLE 2.4

Reaction	K_∞	k_∞ (litre/gm.mole min)	E kcal/gm.mole
I	26,9779	$0{,}520398 \times 10^{12}$	13,8622
II	26,6015	$0{,}357173 \times 10^{12}$	14,1843

Using the above values, reaction rate constants may be obtained which can be compared to those of Meyer and Kremann:-

TABLE 2.5

Temp. °C.	k_1 from above	k_2 from above	k_1 Meyer	k_2 Meyer	k_2 Kremann
0	3,891	1,473	-	1,33	2,5
18	18,98	7,452	15,236	8,089	-
19,8	22,00	8,668	-	9,69	12,5
25	33,38	13,28	32,660	16,312	-

The values of the rate constants obtained in this work show good agreement with those obtained by Meyer, indicating that the latter are more accurate than Kremann's values, and also that the analytical techniques used in this work are sufficiently accurate. The values of k_∞ and E in Table 2.4 were thus used in all further sections of this work to obtain values of rate constants at any temperature.

CHAPTER 3

3.1 POSSIBLE REACTOR TYPES

The three main reactor types in which homogeneous liquid reactions can be carried out are as follows:-

(i) the batch stirred tank reactor

(ii) the continuous stirred tank reactor (CSTR)

(iii) the tubular flow reactor (TFR)

It will be shown later (3.4.1) that the models for the TFR and batch reactor predict identical results, so there would be no special benefits obtained from batch operation. It was thus decided that the optimum reactor would be either a TFR or a CSTR. A batch reactor was used for the majority of the kinetic experiments, however, because these were done in a constant temperature room in which the construction of a continuous flow reactor system would have been impossible due to lack of space for storage vessels and lack of height for obtaining the necessary delivery head.

The mixing in the flow reactors could be on macro or micro scale (Kramers & Westerterp (1963) page 65). In 4.2 it is shown that for reactions I and II below, the ideal TFR is the optimum reactor for macro mixing of reactants. The macro mixed CSTR was thus not considered, and only the ideal CSTR equations were derived.

Since an experimental tubular reactor was built, however, in which both the flow and mixing could be non-ideal, the non-ideal and macro mixed TFR equations were derived as well as those for the ideal TFR.

Mathematical models were thus obtained for the batch reactor, ideal CSTR and ideal, non-ideal and macro mixed TFR.

The nomenclature used for the concentrations of the various species in the reactors is as follows:-

TABLE 3.1

Substance	Initial concentration at time $t=0$ or length $z=0$ gm.mole/litre	Concentration in reactor at time $t=t$ seconds or length $z=z$ cm. gm.moles/litre	Final concentration at time $t=tf$ seconds or length $z=L$ cm. gm.moles/litre
Ethylene glycol diacetate	X_{1o}	X_1	X_{1f}
Sodium hydroxide	X_{2o}	X_2	X_{2f}
Ethylene glycol monoacetate	X_{3o}	X_3	X_{3f}
Sodium acetate	X_{4o}	X_4	X_{4f}
Ethylene glycol	X_{5o}	X_5	X_{5f}

The reactions are given by equations I and II (2.2).

$$\underset{X_1}{\text{Diacetate}} + \underset{X_2}{\text{Caustic}} \xrightarrow{k_1} \underset{X_3}{\text{Monoacetate}} + \underset{X_4}{\text{Sodium acetate}} \qquad \text{I}$$

$$\underset{X_3}{\text{Monoacetate}} + \underset{X_2}{\text{Caustic}} \xrightarrow{k_2} \underset{X_5}{\text{Glycol}} + \underset{X_4}{\text{Sodium acetate}} \qquad \text{II}$$

k_1 and k_2 = reaction velocity constants in litre/gm.mole sec.

As discussed in section 8.1, the concentration of the sodium acetate was not measured for any of the reactor systems, hence only the rates of change of the other species with reactor residence time or reactor length were considered.

As discussed in section 4.3, all reactors were operated iso-

thermally, and thus the inlet concentrations for all reactors were chosen low enough to give less than 1°C temperature rise during mixing and reaction. Hence, for all reactor models discussed, density changes of the reaction mixture due to heating effects were assumed negligible. Due to the low concentrations in the reactor (5.1.2) density changes due to non-ideal behaviour during reaction were also assumed negligible.

3.2 MATHEMATICAL MODEL FOR THE BATCH STIRRED TANK REACTOR

If X_j is the concentration of the jth component in the reaction mixture, in gram mole per litre, then, by mole balance, the rate of change of X_j with residence time, t seconds, in a batch reactor for the above reaction system is given by:-

$$\frac{dX_j}{dt} = \sum_{i=1}^{2} \alpha_{ij} R_i(X_j, T) \qquad j=1,4 \qquad 3.1$$

α_{ij} = stoichiometric coefficient of the jth component in ith reaction (-ve for reactants, +ve for products)

R_i = reaction rate for ith reaction (gm.mole/litre sec)

T = temperature of reaction mixture (°K)

If X_j is written in terms of the initial concentration X_{jo} and the extent of the ith reaction Y_i, then,

$$X_j = X_{jo} + \sum_{i=1}^{2} \alpha_{ij} Y_i \qquad j=1,4 \qquad 3.2$$

Since α_{ij}, $i=1,2$, $j=1,4$ are not identical, differentiating 3.2 and substituting into 3.1 leads to:-

$$\frac{dY_i}{dt} = R_i(X_{jo}, Y_i, T) \qquad i=1,2 \quad j=1,4 \qquad 3.3$$

Using this equation together with the nomenclature in Table 3.1, the batch reactor equations for extents of reaction I, Y_1, and reaction

II, Y_2, above, become:-

$$\left.\begin{aligned}\frac{dY_1}{dt} &= k_1(X_{1o} - Y_1)(X_{2o} - Y_1 - Y_2)\\ \frac{dY_2}{dt} &= k_2(X_{2o} - Y_1 - Y_2)(X_{3o} + Y_1 - Y_2)\end{aligned}\right\} \quad 3.4$$

With boundary conditions

$$Y_{1o} = Y_{2o} = 0 \qquad \text{at } t = 0 \quad 3.5$$

an analytical solution could not be found for equations 3.4, so the modified Euler numerical integration procedure suggested by Lapidus (1962, page 88) was used for their solution.

Once the extents were known as functions of batch reactor residence time, the concentrations of the individual components could be obtained from equation 3.2.

3.3 MATHEMATICAL MODEL FOR THE IDEAL CONTINUOUS STIRRED TANK REACTOR (CSTR)

Using the same nomenclature as in section 3.2 above, from the steady state mole balance for the CSTR:-

$$X_j = X_{jo} + t\sum_{i=1}^{2} \alpha_{ij} R_i(X_j, T) \qquad j=1,4 \quad 3.6$$

where X_j is now the concentration of the jth component of the reaction mixture after a mean residence time of t seconds in the CSTR.

Substituting for the reaction extents from equation 3.2 as before leads to:-

$$Y_i = t\ R_i(X_{jo}, Y_i, T) \qquad i=1,2 \quad j=1,4 \quad 3.7$$

Using this equation and the nomenclature in Table 3.1, the CSTR equations for extents of reactions I and II become:-

$$\left.\begin{aligned}Y_1 &= tk_1(X_{1o} - Y_1)(X_{2o} - Y_1 - Y_2)\\ Y_2 &= tk_2(X_{2o} - Y_1 - Y_2)(X_{3o} + Y_1 - Y_2)\end{aligned}\right\} \quad 3.8$$

3.4 MATHEMATICAL MODELS FOR THE TUBULAR FLOW REACTORS (TFR)

The ideal TFR is the "Plug Flow" or "Piston Flow" reactor in which elements of fluid which enter the reactor at the same moment move through it with constant and equal velocity on parallel paths, and leave at the same moment. The residence time of all elements will thus be equal.

Any deviation from ideality will cause a slowing down of some elements of fluid with respect to the others, and lead to the spread of residence times in the reactor first discussed by Danckwerts (1953). The models for the ideal and non-ideal TFR are discussed below.

3.4.1 Ideal Tubular Flow Reactor (Plug or Pistor Flow Reactor)

If, as in the previous sections, the concentration of the jth component at any length z cm. from the reactor inlet is denoted by X_j gm.mole/litre, then for the plug flow reactor:-

$$\frac{Q'}{a_v}\frac{dX_j}{dz} = \sum_{i=1}^{2} \alpha_{ij} R_i(X_j, T) \qquad j=1,4 \qquad 3.9$$

where

Q' = volumetric flow rate in reactor (cm^3/sec)

a_v = void area in reactor (cm^2)

α_{ij} = stoichiometric coefficient as before

R_i = reaction rate as before.

Hence by substitution of equation 3.2 for the extents of reaction:-

$$\frac{Q'}{a_v}\frac{dY_i}{dz} = R_i(X_{jo}, Y_i, T) \qquad i=1,2 \quad j=1,4 \qquad 3.10$$

Using equation 3.10 plus nomenclature in Table 3.1, the equations for extents become:-

$$\left.\begin{aligned} \frac{Q'}{a_v}\frac{dY_1}{dz} &= k_1(X_{1o} - Y_1)(X_{2o} - Y_1 - Y_2) \\ \frac{Q'}{a_v}\frac{dY_2}{dz} &= k_2(X_{2o} - Y_1 - Y_2)(X_{3o} + Y_1 - Y_2) \end{aligned}\right\} \quad 3.11$$

Boundary conditions

$$Y_{1o} = Y_{2o} = 0 \qquad \text{at } z = 0 \qquad 3.12$$

The residence time in a plug reactor up to any reactor length z is given by:-

$$t = \frac{a_v z}{Q'} \qquad 3.13$$

and substitution of 3.13 into 3.11 will lead to the batch reactor equations 3.4.

Hence the batch and plug flow reactor equations for rate of change of concentration with time are identical. Equations 3.4 and 3.11 were both used for predicting concentration changes in the plug reactor.

3.4.2 Non-Ideal Tubular Flow Reactor

As discussed by Kramers and Westerterp (1963, page 75), non-ideal tubular flow reactors may be considered to be either mixed or segregated systems. Models used to describe the performance of mixed system non-ideal flow reactors are known as "Axial Dispersion" or "Longitudinal Dispersion" models. Segregated reactors are discussed in section 3.4.2.f.

The equation for axial dispersion in a steady state flow reactor is (Danckwerts, 1953):-

$$\frac{D_a}{UL}\frac{d^2X_j}{dZ^2} - \frac{dX_j}{dZ} + \frac{L}{U}\sum_{i=1}^{2} a_{ij}R_i(X_j,T) = 0 \qquad j = 1,4 \qquad 3.14$$

where

D_a = axial dispersion coefficient (cm^2/sec)

X_j = concentration of the jth species at any given z

(gm.mole/litre)

Z = dimensionless length along reactor = z/L

L = total reactor length (cm.)

U = mean fluid velocity in reactor (cm/sec) = Q'/a_v

a_{ij} = stoichiometric coefficient of jth component in ith reaction

R_i = reaction rate of ith reaction (gm.moles/litre sec)

It must be noted that in equation 3.14 D_a has been assumed to be the same for each component. This is because D_a depends on hydrodynamic properties in the bed (see 3.4.2a).

The equation for axial dispersion of a tracer in the unsteady state reactor when there is no reaction, is:- (Danckwerts, 1953; Taylor, 1953, 1954; Kramers & Alberda, 1953),

$$\frac{D_a}{UL}\frac{d^2X}{dz^2} - \frac{dX}{dz} = \frac{L}{U}\frac{dX}{dt} \qquad 3.15$$

where X is now the concentration of the tracer at any point Z in the reactor at any time t.

Equations 3.14 and 3.15 were obtained by analogy to those for molecular diffusion, with the axial dispersion coefficient D_a taking the place of the molecular diffusion coefficient D_m. It can be seen that D_a gives a measure of the degree of axial dispersion present in the reactor. As D_a tends to zero the reactor tends to the plug flow model and as D_a tends to infinity it tends to the CSTR model (Wehner & Wilhelm, 1956). If it is assumed that the dispersion is due to hydrodynamic effects only, then D_a will be the same for both equations, as will U. These equations for the non-ideal tubular reactor have been the subject of many papers:-

(a) Axial Dispersion Coefficient

Taylor (1953, 1954) worked on axial dispersion in stream-

lined flow in tubes. In streamlined flow the parabolic velocity profile in the tube causes a spread of residence times, and hence axial dispersion of the fluid elements. Taylor reasoned that molecular diffusivity in the fluid would tend to even out the concentration gradients caused by axial dispersion. The axial dispersion coefficient, which he called the apparent diffusivity, should thus be inversely proportional to the molecular diffusivity. He was able to prove the following relationship experimentally:-

$$D_a = \frac{r_t^2 U^2}{48\, D_m} \qquad 3.16$$

where

D_a = axial dispersion coefficient (cm^2/sec)

r_t = tube radius (cm)

U = mean fluid velocity (cm/sec)

D_m = molecular diffusion coefficient (cm^2/sec)

Some of the restrictions imposed on the above parameters by Taylor were removed by Aris (1956), who described the distribution of solute in terms of its moments in the direction of flow.

After these papers had been published, many workers attempted to obtain correlations between axial dispersion coefficients and hydrodynamic properties for all possible flow conditions.

Levenspiel (1958) prepared correlation charts for both laminar and turbulent flow of liquids and gases in open tubes. For laminar flow, $\frac{D_a}{Ud_t}$ is correlated against $\frac{Ud_t}{D_m}$ where d_t is the tube diameter. For turbulent flow $\frac{D_a}{Ud_t}$ is correlated directly against Reynolds number $\frac{d_t U \rho}{\mu}$.

Axial dispersion coefficients for liquids and gases in packed beds were obtained by Danckwerts (1953), Kramers and Alberda (1953), McHenry and Wilhelm (1957) and Deisler and Wilhelm (1958). Using this data, correlation charts have been prepared by Levenspiel

and Bischoff (1959), which relate $\frac{D_a}{Ud_p}$ to the Reynolds number in the bed $\frac{d_p U\rho}{\mu}$. Here d_p is the bed packing particle diameter. It will be noted that the parameter occurring in equations 3.14 and 3.15 is $\frac{D_a}{UL}$, where L is the reactor length. Levenspiel and Bischoff show that this may be obtained from:-

$$\frac{D_a}{UL} = \frac{D_a}{Ud_t}\frac{d_t}{L} \qquad 3.17$$

or,

$$\frac{D_a}{UL} = \frac{D_a}{Ud_p}\frac{d_p}{L} \qquad 3.18$$

Wilhelm (1962) gives charts which correlate the Reynolds number based on packing particle diameter against axial Peclet number, given by:-

$$Pe_a = \frac{Ud_p}{D_a} \qquad 3.19$$

The correlations for turbulent flow in open tubes and flow in packed beds are not precise, showing that D_a does not correlate well with hydrodynamic properties in these situations.

(b) Boundary Conditions

The boundary conditions for equations 3.14 and 3.15 have also been the subject of much discussion in the literature. Hulbert (1944) and Danckwerts (1953) each proposed boundary conditions for the equations. The Danckwerts boundary conditions were used by Kramers and Alberda (1953) and Van and Baillie (1960), and Pearson (1959) gave a mathematical justification of them. Wehner and Wilhelm (1956) proposed a new set of boundary conditions for the equations, and these were used by Van der Laan (1958) and Levenspiel and Bischoff (1959). In this last paper equation 3.14 was solved for a range of values of $\frac{D_a}{UL}$ to study the effect of this parameter on the volume of the non-ideal reactor required to perform the same duty as the ideal reactor for first and second order irreversible

reactions.

Finally, Fan and Ahn (1962) presented a critical evaluation of the three sets of boundary conditions outlined above.

The various boundary conditions will now be considered:-

I. Danckwerts:

$$\left.\begin{aligned} (X_j)_{Z=0^-} &= (X_j)_{Z=0^+} - \frac{D_a}{U\Gamma}\left(\frac{dX_j}{dZ}\right)_{Z=0^+} \\ \left(\frac{dX_j}{dZ}\right)_{Z=1} &= 0 \end{aligned}\right\} \quad 3.20$$

II. Hulbert:

$$\left.\begin{aligned} (X_j)_{Z=0^+} &= (X_j)_{Z=0} = (X_j)_{Z=0^-} \\ \left(\frac{dX_j}{dZ}\right)_{Z=1} &= 0 \end{aligned}\right\} \quad 3.21$$

The above boundary conditions have been written for reaction and dispersion, but they will apply to pure dispersion, for which X_j will be replaced by X. Naturally time must be included in the boundary conditions and extra boundary conditions will be required to solve equation 3.15.

III. Semi-Infinite:

In order to obtain these boundary conditions it is assumed that the reactor under consideration constitutes a short length of an infinite reactor, so that Z in equations 3.14 and 3.15 can be allowed to tend to infinity. The boundary conditions will be different for the two differential equations.

Boundary conditions for equation 3.14:-

$$(X_j)_{Z=0^+} = (X_j)_{Z=0} = (X_j)_{Z=0^-}$$

$$(X_j)_{Z=\infty} = 0 \quad \text{if } \sum_i a_{ij} \text{ is negative} \qquad 3.22$$

$$(X_j)_{Z=\infty} = (X_j)_{max} \quad \text{if } \sum_i a_{ij} \text{ is positive}$$

Boundary conditions for equation 3.15:-

$$X_{Z=0^+} = X_{Z=0} = X_{Z=0^-}$$

$$X_{Z=\infty} = \text{finite} \qquad 3.23$$

Fan and Ahn used boundary conditions I, II and III to solve equation 3.14 for varying values of $\frac{UL}{2D_a}$ and $\frac{kL}{U}$, where k is the reaction rate constant. They did this analysis for first, second and third order irreversible reactions, and checked whether the concentration profiles obtained were consistent with the limits of a plug flow reactor and a CSTR.

They found that boundary conditions I gave results which were consistent with these limits, and they also defined regions in $\frac{UL}{2D_a}$ and $\frac{kL}{U}$ space in which II and III are applicable. The inconsistent domain for III was smaller than that for II.

(c) Approach to Ideality

It is evident from both Fan and Ahn's (1962) paper, and that of Levenspiel & Bischoff (1959), that for the majority of tubular reactors, particularly large scale packed industrial reactors, the axial diffusion coefficient will be so low that boundary conditions I, II and III will all yield very similar concentration profiles down the reactor, which will approximate those for the plug flow model very closely. The approach to ideality becomes closer as the length to diameter or length to packing particle diameter ratio in the reactor increases. This approach to ideality is not appreciably affected by the order of the reactions taking place in the reactor.

As an example, consider the case for $\frac{UL}{2D_a} = 20$.

From Figure 3 in Fan and Ahn's work, it can be seen that this value is well within the range of applicability of all three boundary conditions. Their Figures 1, 2, 9 and 10 for concentration profiles down the reactors show that the above value will produce a profile in the non-ideal reactor identical to that in the plug reactor for all cases.

Furthermore, it can be seen from Figures 3 and 4 in Levenspiel and Bischoff's paper, that the above value of $\frac{UL}{2D_a}$, which is equivalent to a value of $\frac{D}{UL}$ of 1/40 leads to a volume difference of roughly 2% between the non-ideal and plug flow reactors for 99% conversion in both a first and second order reaction.

Thus, any reactor in which $\frac{D_a}{UL} \leq 1/40$ can be assumed to obey the plug flow model. The above value has been used together with equations 3.17, 3.18, and the hydrodynamic correlations given by Levenspiel and Bischoff to construct Figure 3.1. On this figure, the shaded areas represent the reactor dimensions for which the reactor will operate ideally. The upper value of $\frac{D}{Ud_t}$, or $\frac{D}{Ud_p}$, was used wherever there was a choice, and since this leads to lower values of $\frac{d_t}{L}$ and $\frac{d_p}{L}$, Figure 3.1 gives the minimum areas for ideal operation.

It is obvious from this figure that all large scale packed bed reactors can be assumed to behave ideally, and that a proportion of open tube turbulent flow reactors will do likewise. Small scale packed beds, turbulent flow reactors operated at low Reynold's numbers and laminar flow reactors will all be non-linear to some degree. The minima obtained in the graphs for the packed beds are due to the scatter of the data obtained by previous workers. This can clearly be seen in Figure 2 in Levenspiel and Bischoff's (1959) paper.

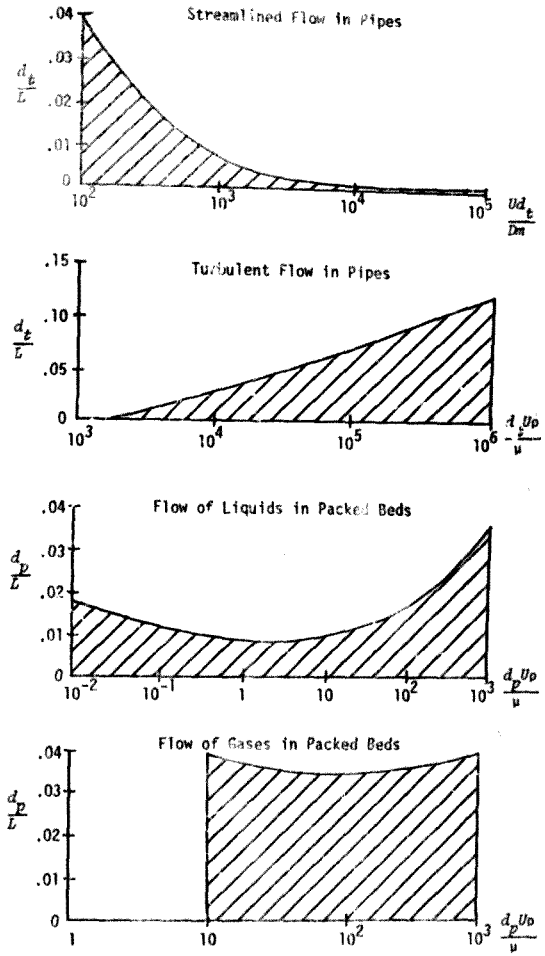

FIGURE 3.1

The shaded areas indicate the regions in which reactor behaviour is ideal.

(d) Axial Dispersion Model and Boundary Conditions for Reactors used in this work

Since this work represents an attempt to approach the design of a reactor in as realistic a fashion as possible, and also since a plug reactor is the optimum for the chosen reaction system (section 4.2) it was decided that this type of flow reactor would be constructed.

The simplest way to do this is obviously to build a packed reactor with a sufficiently low $\frac{d_p}{L}$ ratio. Consequently reactor tubes 150 cm. and 75 cm. long, packed with 0,5 cm. diameter glass beads, were used, giving values of $\frac{d_p}{L}$ of 0,0033 and 0,0066 respectively. The 150 cm. reactor is thus well within the limit of ideality shown in Figure 3.1, while the 75 cm. reactor approaches the limit for Reynolds numbers between 1 and 10 for liquid flow through packed beds.

In order to check the work done by Fan and Ahn and Levenspiel and Bischoff, equation 3.14 was nevertheless solved, using boundary conditions II. From equations 3.2 and 3.14, plus the nomenclature in Table 3.1:-

$$\frac{D_a}{UL}\frac{d^2Y_1}{dZ^2} - \frac{dY_1}{dZ} + \frac{L}{U}k_1(X_{1o} - Y_1)(X_{2o} - Y_1 - Y_2) = 0$$

$$\frac{D_a}{UL}\frac{d^2Y_2}{dZ^2} - \frac{dY_1}{dZ} + \frac{L}{U}k_2(X_{2o} - Y_1 - Y_2)(X_{3o} + Y_1 - Y_2) = 0$$

These can be converted into a system of first order equations by putting:-

$$\left.\begin{aligned} Y_3 &= \frac{dY_1}{dZ} \\ Y_4 &= \frac{dY_2}{dZ} \end{aligned}\right\} \quad 3.24$$

The axial dispersion model equations thus become:-

$$\left.\begin{aligned}
\frac{dY_1}{dZ} &= Y_3 \\
\frac{dY_2}{dZ} &= Y_4 \\
\frac{dY_3}{dZ} &= \frac{UL}{D_a} Y_3 - \frac{L^2}{D_a} k_1 (X_{1o} - Y_1)(X_{3o} - Y_1 - Y_2) \\
\frac{dY_4}{dZ} &= \frac{UL}{D_a} Y_4 - \frac{L^2}{D_a} k_2 (X_{2o} - Y_1 - Y_2)(X_{3o} + Y_1 - Y_2)
\end{aligned}\right\} \quad 3.25$$

Y_1 = extent of reaction I (gm.moles/litre) } section 3
Y_2 = extent of reaction II (gm.moles/litre) }

Y_3 } defined by equation 3.24
Y_4 }

Z = dimensionless reactor length x/L

L = total reactor length (cm)

U = mean velocity of flow in reactor (cm/sec)

D_a = axial, longitudinal, apparent or Taylor dispersion coefficient (cm^2/sec)

k_1 = reaction rate of reaction I

k_2 = reaction rate of reaction II

X_{1o} }
X_{2o} } initial concentrations as defined in Table 3.1
X_{3o} }

The boundary conditions obtained similarly from equations 3.21 are:-

$$\left.\begin{aligned}
Y_{1o} = Y_{2o} &= 0 \qquad Z=0 \\
Y_{3f} = Y_{4f} &= 0 \qquad Z=1
\end{aligned}\right\} \quad 3.26$$

(e) Estimation of Parameters for the Axial Dispersion Model

L was known for the reactor, but before equations 3.25 could be solved, values of U and D_a had to be obtained. Due to the lack of precision in the various correlations for D_a (3.4.2.a), it was

decided that these parameters would be measured experimentally.

Levenspiel and Smith (1957) give a method for obtaining D_a and U by injecting tracer pulses into the column inlet and using equation 3.15 to fit the outlet response concentration-time curve. They use the semi-infinite boundary conditions 3.23, which are not the same as those used to solve the reactor equation 3.14 in this work. However, it was expected that all the boundary conditions would give the same result (3.4.2.c.), and use of different boundary conditions for equations 3.14 and 3.15 will serve to demonstrate whether or not these expectations were justified.

As stated earlier, (3.4.2.b.), the boundary conditions 3.23 have to be augmented by one, and have to include time t before equation 3.15 can be solved. The augmented semi-infinite boundary conditions for a pulse injected into the reactor inlet at time $t=0$ thus become:-

$$\left.\begin{array}{lll} Z = 0 & X = \delta(t) & t = 0 \\ Z > 0 & X = 0 & t = 0 \\ Z = \infty & X = \text{finite, therefore } \frac{dX}{dZ}=0 & t > 0 \end{array}\right\} \quad 3.27$$

where

$\delta(t)$ = unit dirac delta function

The reactor output curve will correspond to the "C diagram" given by Danckwerts (1953) and if this is normalised, the normalised curve will correspond to the response to a unit impulse input, i.e. Danckwerts' exit age (residence time) distribution function, $E(t)$, for which:-

$$\int_0^\infty E(t)dt = 1 \quad 3.28$$

Levenspiel and Smith (1957) have shown that for equation 3.15 and boundary conditions 3.27, the mean, variance and skewness of the $E(t)$ curve can be related to the parameters U, D_a and L as

follows:-

$$\text{Mean} = \frac{L}{U}$$

$$\text{Variance} = \frac{2LD_a}{U^3} \qquad 3.29$$

$$\text{Skewness} = \frac{12LD_a^2}{U^5}$$

Using moment generating functions (Kwitz, 1961) to characterise the $E(t)$ curve, it can be shown that:-

$$\text{Mean} = \frac{\int_0^\infty tE(t)dt}{\int_0^\infty E(t)dt} = \int_0^\infty tE(t)dt$$

$$\text{Variance} = \int_0^\infty t^2E(t)dt - \left(\int_0^\infty tE(t)dt\right)^2 \qquad 3.30$$

$$\text{Skewness} = \int_0^\infty t^3E(t)dt - 3\left(\int_0^\infty t^2E(t)dt\right)\left(\int_0^\infty t^3E(t)dt\right) + 2\left(\int_0^\infty tE(t)dt\right)^3$$

The experimental procedure used for obtaining the $E(t)$ curves is discussed in section 6.1. Equations 3.29 and 3.30 were used to solve for D_a and U. The skewness was used as a check on the values obtained from the mean and the variance.

The values of D_a and U obtained were substituted into equations 3.25 and these were solved on an IBM 360/50 computer, with boundary conditions 3.26 using Glasser's (1969) numerical solution of two point boundary value problems. The results are discussed in Chapter 9.

An additional check on the dispersion model and boundary conditions was carried out as follows. The dispersion equation 3.15 with these calculated values of D_a and U, was solved using Laplace Transforms and the numerical inversion technique derived by Bryson

and co-workers (1971) to see if the experimental $E(t)$ curves could be reconstituted.

(f) Segregated Flow Model

In the above models, it has been assumed that the reactants were well mixed on entering the reactor, and that the reaction mixture remained chemically uniform while passing through the reactor (3.4.2).

Danckwertz (1957) and Zwietering (1959) raised the possibility of another mixing mechanism, in which the incoming fluid is broken up into discrete fragments which retain their identity while passing through the reactor. This postulation leads to the segregated flow model for the reactor. It is possible to obtain segregated flow in both a CSTR and a TFR.

The segregated flow reactor may thus be considered to be made up of a number of non-interacting batch reactors. The residence times in these batch reactors will vary depending on the flow conditions in the reactor, and the concentration in the exit stream from the segregated flow reactor can be obtained by determining the extent of reaction in each of the batch reactors.

Hence, from Levenspiel (1962, page 312):-

$$X_{jf} = \int_0^\infty (X_j)_{batch} E(t)dt \qquad 3.31$$

where X_{jf} = final concentration of component j in a segregated flow reactor (= concentration of component j in exit stream)

$(X_j)_{batch}$ = batch reactor concentration of component j after any residence time t

$E(t)$ = residence time distribution function

Equation 3.31 was integrated using the Modified Euler pro-

cedure (Lapidus (1962) page 88) and the batch reactor equations (see 3.2). Since both an experimental and a calculated residence time distribution were available, both were used to obtain final concentrations from equation 3.31.

Once the results had been obtained, they could be compared to the experimental final concentrations to see whether or not the flow in the reactor was segregated.

3.5 SUMMARY OF MATHEMATICAL MODELS AND CALCULATIONS

Mathematical models were developed for the batch reactor, the continuous stirred tank reactor, and the ideal and non-ideal tubular flow reactor. It was found that the batch and ideal tubular flow reactor models were identical. For the non-ideal tubular flow reactor, the axial dispersion model was obtained, together with suitable boundary conditions and methods of evaluating the parameters in this model. The mathematical analysis leads one to expect that the ideal and non-ideal tubular flow reactor models should yield results differing by not more than 2%, for the reactor in this work.

The segregated flow model was also obtained, together with a method of obtaining exit concentrations from this model.

All of the models were solved using an IBM 360/50 computer, and the results and discussions are given in Chapter 9.

CHAPTER 4

4.1 CHOICE OF OBJECTIVE FUNCTION

The system of reactions is:-

$$\underset{X_1}{\text{Diacetate}} + \underset{X_2}{\text{sodium hydroxide}} \xrightarrow{k_1} \underset{X_3}{\text{monoacetate}} + \underset{X_4}{\text{sodium acetate}} \qquad \text{I}$$

$$\underset{X_3}{\text{Monoacetate}} + \underset{X_2}{\text{sodium hydroxide}} \xrightarrow{k_2} \underset{X_5}{\text{ethylene glycol}} + \underset{X_4}{\text{sodium acetate}} \qquad \text{II}$$

In the above system, monoacetate represents the desired intermediate product and glycol and sodium acetate the undesired end products. It was thus decided that the monoacetate concentration, X_3, would be maximised in this work. The objective or profit function, N, is then defined by:-

$$N = AX_{3f} \qquad 4.1$$

where A is a positive constant relating X_3 to profit. This is thus a yield problem, as defined by Denbigh (1958), and consists of choosing the operating conditions which maximise N.

4.2 OPTIMUM REACTOR DESIGN

It was decided in 3.1 that either a TFR (tubular flow reactor) or a CSTR (continuous stirred tank reactor) could be used, with the possibility of micro or macro mixing in either of these reactors. For macro mixing, the flow in the reactor would be segregated, and the reactor could be assumed to consist of a number of batch reactors in parallel. Each of these batch reactors would have a residence time associated with it.

Due to the fact that monoacetate is formed in reaction I

above, and consumed in reaction II, there would be an optimum residence time in a batch reactor for which X_{3f} would be a maximum. If the flow in the CSTR or TFR is segregated, therefore, the flow conditions should be chosen such that each fluid element resides in the reactor for the optimum residence time. Any spread of residence times would cause fluid elements at a concentration below the optimum to leave the reactor together with elements at the optimum concentration and so reduce the resulting outlet value of X_{3f} to below the optimum. This means that if there was macro mixing of reactants, the optimum type of reactor would be the ideal TFR. Any other type of reactor would lead to a spread of residence times in the segregated streams, which would result in X_{3f} being below the maximum.

It was found that a similar deduction could not be made for micro mixing of the reactants, but it is likely that the ideal TFR will also be the optimum due to the spread of residence times of individual molecules in the CSTR and non-ideal TFR. In order to test this supposition, the CSTR and ideal TFR models derived in 3.3 and 3.4 were solved to give values of X_3 versus time, using the same inlet concentrations and temperatures for each model. It will be seen from Chapter 9 that the ideal TFR model led to consistently higher maximum values of X_3 than the CSTR.

It was thus assumed for this work that the ideal TFR or plug flow reactor was the optimum type of reactor.

4.3 CHOICE OF OPTIMUM OPERATING CONDITIONS FOR THE PLUG REACTOR

The choice of an optimum temperature policy will be considered first.

By substituting equation 3.13 into equation 3.9, the minimum number of state equations defining the plug flow reactor system can be obtained:-

$$\left.\begin{aligned} \frac{dX_1}{dt} &= -k_1X_1X_2 \\ \frac{dX_3}{dt} &= k_1X_1X_2 - k_2X_2X_3 \end{aligned}\right\} \quad 4.2$$

Equations 4.2 constitute two linearly independent differential equations with boundary conditions:-

$$t = 0, \quad X_1 = X_{1o}, \quad X_2 = X_{2o}, \quad X_3 = 0 \quad 4.3$$

From equation 2.1

$$\left.\begin{aligned} k_1 &= k_{\infty 1}exp(-E_1/RT) \\ k_2 &= k_{\infty 2}exp(-E_2/RT) \end{aligned}\right\} \quad 4.4$$

Since $k_1>0$ except in the boundary case where $T=0$, and since the yield problem is being considered, for which M is a function of the state variables only, and not t, (see 4.1), the following substitutions can be made:-

Set $$K = \frac{k_2}{k_1} = \frac{k_{\infty 2}}{k_{\infty 1}} exp\{\frac{E_1 - E_2}{RT}\} \quad \text{(from 4.4)} \quad 4.5$$

and $$d\tau = k_1dt, \qquad \tau = 0 \text{ when } t = 0 \quad 4.6$$

Hence

$$\left.\begin{aligned} \frac{dX_1}{d\tau} &= -X_1X_2 \\ \frac{dX_3}{d\tau} &= X_1X_2 - KX_2X_3 \end{aligned}\right\} \quad 4.7$$

With boundary conditions:- $\tau = 0, \quad X_1 = X_{1o}, \quad X_2 = X_{2o}, \quad X_3 = 0$ 4.8

As discussed in 4.1, the objective function is:-

$$M = AX_{3f} \quad 4.1$$

The problem thus becomes to maximise M by suitable choice of temperature policy. In the state equations 4.7, K is the only variable which is an explicit function of temperature. From 4.5 K is a monotonic function of temperature, hence K can become the control and the problem is to maximise M by suitable choice of K, i.e.:-

$$\max_K M = X_{3f} \quad 4.9$$

This is a variational problem and Pontryagin's Maximum Principle (1962) was used to obtain the optimum control policy.

Applying the Maximum Principle, a necessary condition for 4.9 is:-

$$\max_{K} H \qquad 4.10$$

where H is the Hamiltonian for the system and is given by:-

$$H = X_1 X_2(\lambda_2 - \lambda_1) - KX_2X_3\lambda_2 \qquad 4.11$$

where λ_1 and λ_2 are the adjoints defined by the equations below. From 4.11 it will be seen that H is linear in the control K. Further $X_2X_3>0$ except in the boundary cases where $\tau = 0$ or ∞.

Hence in order to apply 4.10:-

If $\lambda_2>0$, K must be set at its minimum value (bang bang control)
If $\lambda_2<0$, K must be set at its maximum value (bang bang control) 4.12
If $\lambda_2=0$, and $\frac{d\lambda_2}{d\tau} = 0$, K must be set at some intermediate value (intermediate control)

The adjoint equations are:-

$$\frac{d\lambda_1}{d\tau} = -\frac{\partial H}{\partial X_1} = X_2(\lambda_1 - \lambda_2)$$
$$\frac{d\lambda_2}{d\tau} = -\frac{\partial H}{\partial X_3} = KX_2\lambda_2 \qquad 4.13$$

Transversality condition:-

$$\frac{\partial M}{\partial X_{1f}} = \lambda_{1f} \qquad \frac{\partial M}{\partial X_{3f}} = \lambda_{3f}$$

Hence boundary conditions for the adjoint equations are:- (from 4.1)

$$\tau = \tau f \qquad \lambda_{1f} = 0 \qquad \lambda_{3f} = A \qquad 4.14$$

where τf corresponds to $t=tf$

Integrating 4.13 and applying the boundary condition 4.14:-

$$\lambda_2 = A\exp(-\int_T^{Tf} X_2 K dT) \qquad 4.15$$

Now $A\exp(-\int_T^{Tf} X_2 K dT) > 0$ for all admissible A, X_2, K and T.

Hence except for the boundary case where $Tf = \infty$,

$$\lambda_2 > 0 \qquad 4.16$$

From 4.12 and 4.16, it is evident that bang bang control is optimal, and that in order to maximise M, K must be minimised by suitable choice of temperature.

From 4.5:-

$$K = \frac{k_{o2}}{k_{o1}} \exp\left(\frac{E_1 - E_2}{RT}\right)$$

In order to minimise K:-

If $E_1 > E_2$, T must be set at its maximum value

If $E_1 < E_2$, T must be set at its minimum value

If $E_1 = E_2$, the maximum value of M is not dependent on temperature.

The reactor must thus be operated isothermally at either the highest or the lowest possible temperature depending on the respective activation energies of the two reactions.

Since the reactions take place in liquid medium, pressure would not have a direct effect on the reaction rate, but would obviously influence the maximum attainable temperature before a phase change occurs.

As can be seen from Table 2.4, the activation energies are:-

E_1 = 13,5622 kcal/gm.mole

E_2 = 14,1843 kcal/gm.mole

Hence the reaction temperature should be kept as low as possible

$$\lambda_2 = A\exp(-\int_{T}^{Tf} X_2 K dT) \qquad 4.15$$

Now $A\exp(-\int_{T}^{Tf} X_2 K dT) > 0$ for all admissible A, X_2, K and T.

Hence except for the boundary case where $Tf = \infty$,

$$\lambda_2 > 0 \qquad 4.16$$

From 4.12 and 4.16, it is evident that bang bang control is optimal, and that in order to maximise M, K must be minimised by suitable choice of temperature.

From 4.5:-

$$K = \frac{k_{=2}}{k_{=1}} \exp\left(\frac{E_1 - E_2}{RT}\right)$$

In order to minimise K:-

If $E_1 > E_2$, T must be set at its maximum value

If $E_1 < E_2$, T must be set at its minimum value

If $E_1 = E_2$, the maximum value of M is not dependent on temperature.

The reactor must thus be operated isothermally at either the highest or the lowest possible temperature depending on the respective activation energies of the two reactions.

Since the reactions take place in liquid medium, pressure would not have a direct effect on the reaction rate, but would obviously influence the maximum attainable temperature before a phase change occurs.

As can be seen from Table 2.4, the activation energies are:-

E_1 = 13,8622 kcal/gm.mole

E_2 = 14,1843 kcal/gm.mole

Hence the reaction temperature should be kept as low as possible

to maximise M. Since the difference between E_1 and E_2 is small, however, the effect of temperature on the maximum value would not be great, so no attempt was made to optimise M experimentally by choice of reaction temperature.

It was decided that the reactor would be operated isothermally at atmospheric pressure and as close to room temperature as possible while still maintaining constant inlet temperatures of reactants.

CHAPTER 5

5.1 CHOICE OF OPERATING CONDITIONS

5.1.1 Operating Temperature

In section 4.3 it can be seen that the reactor was to be operated isothermally. It was decided that this would be done as close to room temperature as possible. Heaters and thermostats were installed for the feed tanks so that the inlet temperatures could be controlled at 3-4°C above room temperature. The resulting temperature range for the runs was 21-26°C.

5.1.2 Inlet Concentration

From the discussion of the batch reactor experiments in 2.3.2, it will be seen that the diacetate and caustic soda were fed to the reactors in stoichiometric ratios. Further, the upper and lower limits of diacetate concentration were 0,1 and 0,005 molar respectively. The feeds to the main reactor were thus kept in stoichiometric proportions too, with diacetate inlet concentration being held between these limits.

5.1.3 Flowrates

The diacetate and caustic soda solutions were supplied to the reactor inlet by gravity feed. The pressure drops in the supply tubing, inlet mixing section and the reactor packing thus set the upper limit on the reactor flowrate. It was found from experiments with water flowing through the column that with both streams flowing, the maximum flowrate was 4 litres per minute. Hence the upper limit in each feed stream was 2 litres per minute. The Fischer-Porter flowmeters chosen for this work delivered a maximum of 1,8, and a minimum of 0,18 litres per minute. In practice it was found that the maximum and minimum inlet flow of each stream which could be

obtained were 1,65 and 0,38 litres per minute (see Appendix i). The inlet flowrate could thus be varied from 3,30 to 0,76 litres per minute, corresponding to column residence times of 26,8 to 116,2 seconds for the long reactor, and 13,1 to 56,5 seconds for the short reactor.

Solving the plug flow model with these residence times and the inlet concentrations given above, at 23°C, it was found that conversions of diacetate (see 2.3.2) from 15% to 98% could be obtained in the reactor. It was felt that these spanned the conversion range sufficiently to give a good test of the mathematical models.

5.2 LAYOUT AND CONSTRUCTION OF THE REACTOR SYSTEM

Figure 5.1 shows the layout of the experimental plug flow reactor system. Figure 5.2 gives a flowsheet for the system. The figures are not drawn to scale, and for clarity the sample points and drainage lines required to remove air bubbles from the system have been omitted. A photograph of the apparatus is given on the following page.

5.2.1 Feed System and Temperature Control

The stock tanks were polythene, had a capacity of approximately 800 litres, and were mounted on a gallery 10 metres above the reactor inlet. They were stirred at 725 r.p.m. The diacetate and caustic soda feed tanks each had four 1 kw. electric wall mounted heaters. The current supply to these was controlled by an on-off thermostat which could be used to regulate the feed-stock temperatures to within 1°C. (The makes and model numbers of all equipment used are given in the equipment list in Appendix xi).

There was no need to regulate the temperature of the acetic acid solution since this was simply used to quench the reaction mixture at the reactor outlet.

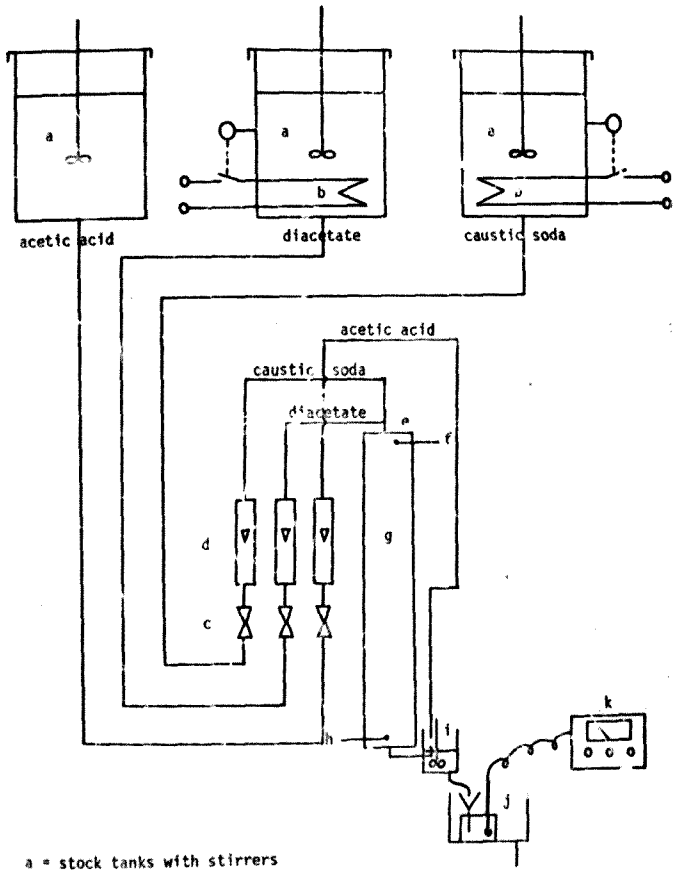

a = stock tanks with stirrers
b = thermostats and heaters
c = flow control valves
d = flowmeters
e = inlet mixing section
f = inlet thermometer
g = packed bed reactor
h = outlet thermometer
i = outlet quench section
j = pH measuring electrode and beaker
k = pH meter

FIGURE 5.1

Plug Flow Reactor System

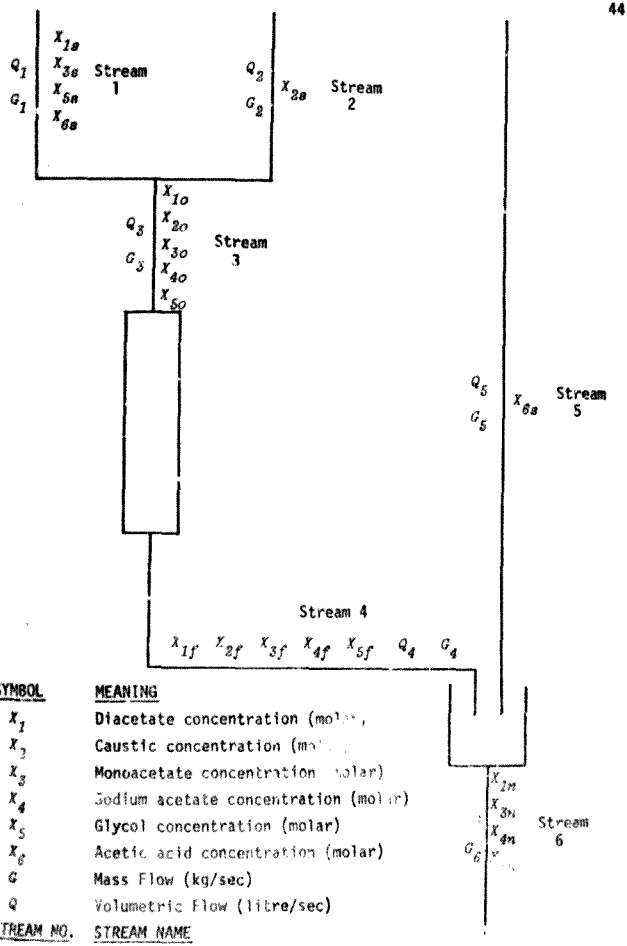

SYMBOL	MEANING
X_1	Diacetate concentration (molar)
X_2	Caustic concentration (molar)
X_3	Monoacetate concentration (molar)
X_4	Sodium acetate concentration (molar)
X_5	Glycol concentration (molar)
X_6	Acetic acid concentration (molar)
G	Mass Flow (kg/sec)
Q	Volumetric Flow (litre/sec)

STREAM NO.	STREAM NAME
1	Diacetate Feed
2	Caustic Feed
3	Reactor Inlet
4	Reactor Outlet
5	Quench Acetic Acid
6	Neutralised Stream

FIGURE 5.2

The lines from the feed tanks to the control valve and the inlet connecting pieces were 25,4 mm. diameter flexible PVC. All other lines were 12,7 mm. diameter rigid PVC.

5.2.2 Flow Control and Measurement

The flow of all three solutions was regulated by 12,7 mm. diameter stainless steel needle valves, and as mentioned above, Fischer Porter Flowrator meters were used to meter the flows. It was decided that rotameters would be used in preference to orifice plates because the former are self-cleaning and insensitive to the presence of flow obstructions up and downstream from them. The Fischer Porter meters were chosen because they have a degree of viscosity immunity and are thus not affected by small temperature changes in the liquid (Fischer and Porter, 1968).

5.2.3 Inlet Mixing Section

The inlet mixer proved to be the most critical section of the whole reactor. Both inlet mixers used in this work are shown in Figure 5.3. They were fitted with O ring seals, and clamped into the top of the reactor. Both were filled with beads to reduce the residence time in them to a minimum.

Initially it was thought that the T-piece mixer would not be efficient at low flow rates, and consequently experiments were carried out at the low flow rates to check the efficiency of mixing. Tracers of dye were injected into each of the inlet lines in turn with water flowing in both of them. The mixing seemed to be instantaneous, the liquid appearing homogeneous with no dye streams visible. These experiments were repeated later with a concentrated dye solution in one stream and water in the other, and the fluids still appeared perfectly mixed. When the main runs were carried out, however, it was found that the inlet mixing at low flow rates

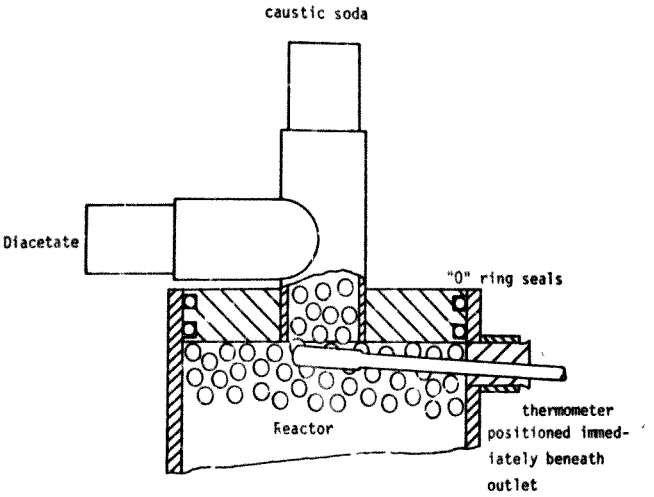

FIGURE 5.3.1
T-Piece Inlet

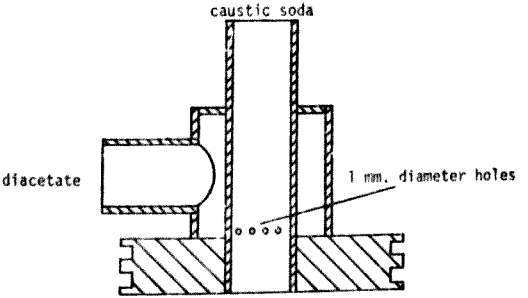

FIGURE 5.3.2
Ring Inlet

was extremely poor and subsequent measurements with a conductivity probe confirmed this (see Appendix iii). The second inlet mixer shown in Figure 5.3.2 was then made up. This mixer had a considerably greater pressure drop across it, but the inlet mixing was greatly improved.

5.2.4 Reactor

The reactor was constructed from 63,5 mm. O.D., 50,8 mm. I.D. perspex since this was readily available and chemically inert. As discussed in 3.4.2(d), the lengths of reactor used were to have been 150 cm. and 75 cm. When the units had been fabricated, the actual lengths were found to be 149,8 cm. and 73,0 cm. The reactor was packed randomly with 5 mm. diameter glass beads. The holdup volume for the 149,8 cm. length was found to be 1,472 litres, and that for the 73,0 cm. length was found to be 0,716 litres. (See 6.6 and Appendix v).

The inlet and outlet thermometers were fitted through bosses on the reactor walls with rubber bungs. Both thermometers were 61 cm. long, calibrated in 0,01°C. The thermometer bosses were used for the conductivity probe when testing the inlet mixing system.

5.2.5 Reactor Outlet and Outlet Quench Vessel

The reactor outlet pipe consisted of a very short 12,7 mm, diameter rigid PVC U-bend which terminated in the quench vessel. It was found that a U-bend pointing vertically upwards was necessary on the reactor outlet, or else the reactor would drain as soon as the flows were turned off. For the same reason it was necessary to have a U-bend on the acetic acid quench pipe.

In order to prevent accidental draining of the column, a rubber bung was fitted to this outlet whenever the column was not in use or when the drainage lines were open to remove air bubbles from the system.

A detailed sketch of the reactor outlet and the outlet quench vessel is given in Figure 5.4. It can be seen from this that every effort was made to obtain rapid quenching of the outlet stream. Originally the quench stream joined the reactor outlet via a T-piece but it was found with this arrangement that all three flows interacted, and it was impossible to regulate them so as to obtain the correct pH of the quenched solution. The quench vessel was stirred at 960 r.p.m., and although the liquid level was 1.75 cm., the vessel was 25 cm. high to prevent splashing out.

5.2.6 pH Measurement and Rotameter Calibration

From the quench vessel the quenched solution flowed via a flexible tube into a funnel and thence into a beaker where the pH could be measured.

Originally the pH electrodes were placed directly in the outlet quench vessel, but it was found that slugs of air stirred into the quenched solution made it impossible to read the pH. The liquid leaving the quench vessel also carried the slugs with it, so the funnel was provided to reduce the liquid velocity and enable the air to escape before the pH was measured in the beaker. Once the system was at steady state, the pH in the quench vessel and beaker were the same. This system was tested and found to work within the limits of experimental accuracy (see Appendix iv). The pH electrode was combined with a temperature compensator so that the pH meter did not have to be re-zeroed for different outlet temperatures.

The outlet tube from the quench vessel was made flexible to allow the flow to be switched from the funnel to a measuring cylinder for flowmeter calibrations.

A summary of the reactor and the outlet quench vessel dimensions is given in Table 5.1, together with the maximum and minimum residence times and flow rates in each.

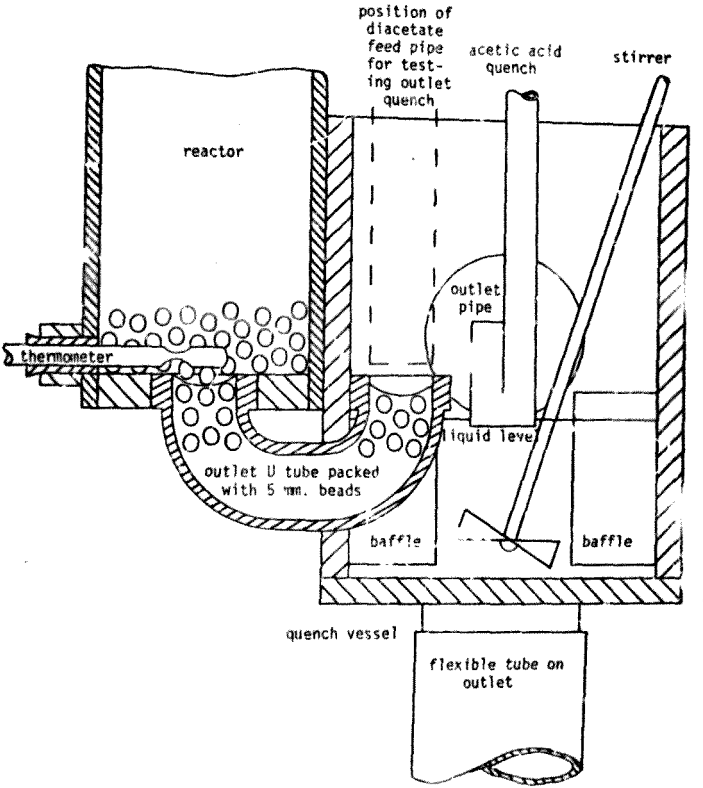
position of diacetate feed pipe for testing outlet quench
acetic acid quench
stirrer
reactor
outlet pipe
thermometer
liquid level
outlet U tube packed with 5 mm. beads
baffle
baffle
quench vessel
flexible tube on outlet

FIGURE 5.4

TABLE 5.1

	Reactor		Outlet Quench Vessel
Material	perspex		PVC
O.D.	63,5 mm.		101,6 mm.
Wall thickness	6,35 mm.		7,44 mm.
Length	149,8 cm.	73,0 cm.	25 cm.
Holdup volume	1,472 litre	0,716 litre	0,245 litre
Packing	5mm. diameter glass beads		-
Liquid level	-		1,75 cm.
Maximum flowrate	3,3 litre/min.		3,3 litre/min.
Minimum flowrate	0,76 litre/min.		0,76 litre/min.
Maximum residence time	116,2 sec.	56,5 sec.	19,3 sec.
Minimum residence time	26,8 sec.	13,1 sec.	4,5 sec.

CHAPTER 6

6.1 EXPERIMENTAL TECHNIQUES

As discussed in 3.4.2.e, an experimental technique was required to obtain the exit age distribution function $E(t)$ for the reactor at various flowrates, so that this function could be used to obtain values of mean velocity U, and axial dispersion coefficient, D_a, for the reactor. The $E(t)$ function was also required for the solution of the segregated flow model in section 3.4.2.f.

If a tracer pulse is injected into the column inlet, the exit concentration function $C(t)$ discussed by Danckwerts (1953) will be obtained at the reactor outlet. The exit age distribution function $E(t)$ can be obtained by normalising the $C(t)$ function, and Levenspiel and Smith's (1957) method can then be used to obtain D_a and U.

The tracer used in this work was 175 gm./litre sodium chloride solution. This was chosen because sodium chloride concentration is proportional to conductivity and a conductivity meter was available which could be connected to a pen recorder to trace out the exit age distribution curve. (Makes and model numbers of all instruments are given in Appendix xi).

It was found experimentally that with pure water flowing in the column, the maximum volume of tracer required was 0,5 cm^3. This volume could be injected in under 0,2 seconds. Since the minimum residence time in the long column was 27 seconds, it was assumed that a perfect pulse could be injected. The tracer was thus injected into the flexible reactor inlet lines with a hypodermic syringe, and a 1 cm. standard conductivity cell was fitted into the reactor outlet pipe by means of a rubber stopper.

From 5.2.3, it will be seen that two different inlet mixing systems were used for the reactor. It was not known how the residence time distribution would be affected by these inlets so $E(t)$ curves were obtained for both. Eighteen runs spanning the flowrate range were carried out with the T-piece mixer, Figure 5.3.1. For all of these runs, the tracer was injected into the straight run inlet of the T, with distilled water flowing in both inlets. Ten runs spanning the flowrate range were done with the ring mixer, Figure 5.3.2, and for half of these the tracer was injected into the straight run, and for the other half it was injected into the side inlet. The results should thus show the effect of the inlet system and injection point on the residence time distribution.

Table 6.1 lists flowrates and injection points for each run, together with the values of D_a and U obtained. These runs were only carried out on the 149.8 cm. reactor length since it was felt that the residence times would be too short in the 73 cm. length. The Taylor model was thus not solved for the short reactor.

6.2 LINEARITY OF CONDUCTIVITY METER

Sodium chloride solutions of varying concentrations were made up, the cell was placed in them, and the recorder reading was noted. The resulting graph of concentration versus potential is given in Figure 6.1. From the graph, it can be seen that the entire system is linear, and that the recorder output gives a measure of concentration. The recorder traces were thus taken as the concentration-time curves for these experiments.

6.3 MATHEMATICAL PROCEDURES (see 3.4.2.e)

The experimental data obtained during these runs are listed in Appendix viii. These were stored on the IBM 360/50 computer, and

TABLE 6.1

Run No.	Inlet Type	Injection Point	Flowrate (litre/min)	U cm/sec	D_a cm^2/sec
1	T	Straight run	0,5509	0,9371	0,9012
2	T	Straight run	0,5509	0,9360	0,9623
3	T	Straight run	0,7819	1,320	1,474
4	T	Straight run	0,7819	1,305	1,243
6	T	Straight run	1,1944	2,013	1,796
7	T	Straight run	1,5613	2,617	2,492
8	T	Straight run	1,5613	2,637	2,256
9	T	Straight run	1,9257	3,276	2,780
10	T	Straight run	1,9257	3,266	2,829
11	T	Straight run	2,2851	3,882	3,179
12	T	Straight run	2,2851	3,881	3,282
13	T	Straight run	2,6450	4,462	3,823
14	T	Straight run	2,6450	4,490	3,783
15	T	Straight run	2,9940	5,045	4,403
17	T	Straight run	2,9924	5,100	4,095
18	T	Straight run	3,3342	5,676	4,470
19	T	Straight run	3,3342	5,674	4,613
20	T	Straight run	3,3342	5,672	4,360
27	Ring	Side branch	0,4878	0,8315	0,901
28	Ring	Straight run	0,4878	0,8618	1,039
29	Ring	Side branch	1,2018	2,055	1,918
30	Ring	Straight run	1,2018	2,019	2,551
31	Ring	Side branch	1,9584	3,378	2,659
32	Ring	Straight run	1,9584	3,332	2,807
33	Ring	Side branch	2,6694	4,549	3,540
34	Ring	Straight run	2,6694	4,554	3,589
35	Ring	Side branch	3,3374	5,654	4,921
36	Ring	Straight run	3,3374	5,749	4,960

Note: Runs 5 and 16 were discarded due to excessive baseline drift. Runs 21-26 were discarded because the recorder was overdamped and the $E(t)$ curves were affected by the recorder dynamics.

CONDUCTIVITY CELL CALIBRATION CURVE

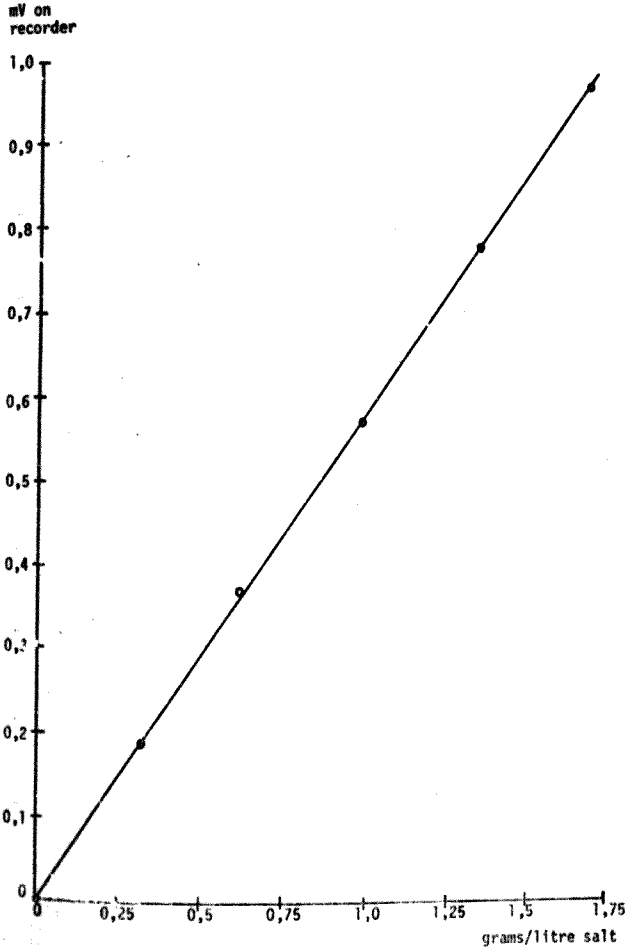

FIGURE 6.1

used as inputs to a program which:-

(a) normalised the recorder trace so as to get the $E(t)$ curve and stored this as a new data set;

(b) calculated the mean, variance and skewness of the $E(t)$ curve;

(c) used the mean and variance to calculate the liquid velocity U and axial dispersion coefficient, D_a;

(d) used the skewness to check the value of D_a obtained in (c).

The record length and time intervals of the original traces plus the values of D_a and U calculated in (c) were fed as data to a program which solved the diffusion equation 3.15 (section 3.4.2), to give a theoretical $E(t)$ curve - this curve was also stored as data.

One of the output devices attached to the computer used in this work is a Calcomp plotter, by means of which output data can be obtained directly in graphical form. A further program was thus used to combine the experimental and theoretical $E(t)$ data and plot them on the same axes using this plotter.

The experimental and theoretical $E(t)$ curves were also used as input data to a program which solved the segregated flow models for the reactor (3.4.2.f).

6.4 RESULTS

The velocities and axial dispersion coefficients obtained for the experiments are given in Table 6.1 and plotted in Figures 6.2 and 6.3. The method given by Mickley Sherwood and Reed (1957, pages 95-96) was used to obtain the least squares straight lines through the data. The equations to the lines were:-

$U = 1,694Q$ with a variance of estimate of 0,00106 6.1

$D_a = 0,344 + 1,383Q$ with a variance of estimate of 0,0390 6.2

U = velocity (cm./sec.)

D_a = axial dispersion coefficient (cm^2/sec.)

Q = volumetric flow (litres/min.)

Figures 6.4-6.16 are the $E(t)$ curves drawn by the Calcomp plotter. The $E(t)$ curve obtained by normalising the experimental $C(t)$ curve (see 6.3.a,) is marked by triangles which were drawn in at every thirtieth actual experimental point. These curves are for low, medium and high flowrates, and the injection points for each can be obtained from Table 6.1.

Similar curves to the above were obtained for all the experimental runs, so Figures 6.4-6.16 may be regarded as representative of these.

6.5 DISCUSSION

It was found for all runs that the skewness of the $E(t)$ curve did not yield reproducible values of D_a. Values of U and D_a in Figures 6.2 and 6.3, therefore, were obtained from the mean and variance only.

In 6.1 it will be seen that the inlet mixing devices and injection points were varied during the runs. The extremely low value of the variance of estimate obtained for the U data therefore proves that the mean of the residence time distribution is not affected by the inlet mixing or by the inlet injection point. It also shows that the injection time was negligible compared to the mean column residence time.

It should be noted that there was a time interval of two years between the sets of runs with the two different inlets, and that the column was unpacked and repacked approximately eight times during this period. The fact that reproducible values of U were still obtained indicates that the column packing was truly random,

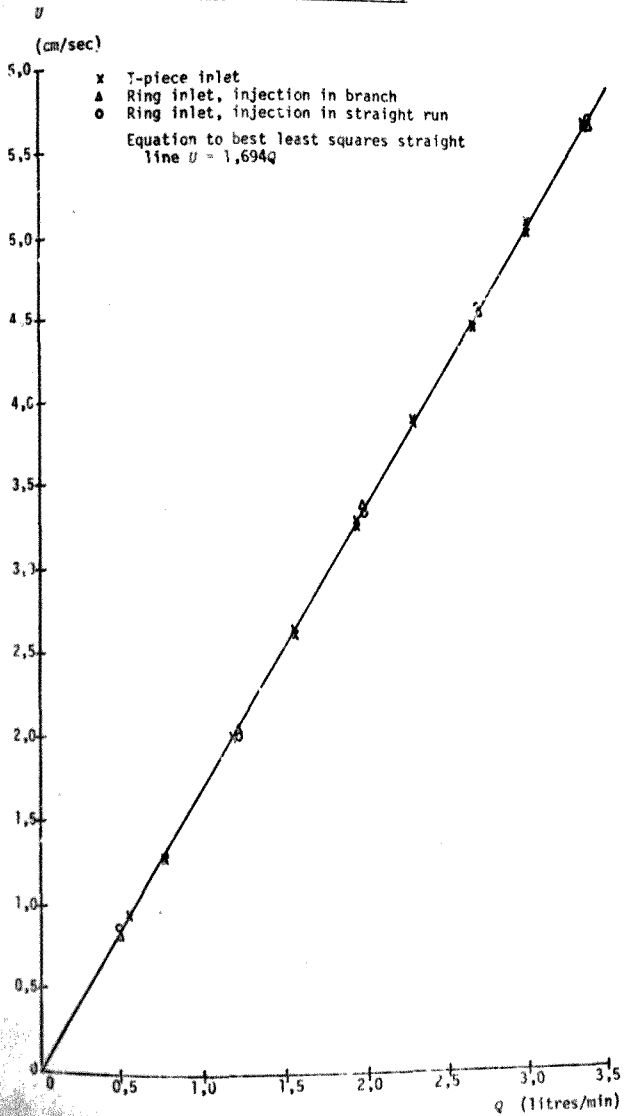
VELOCITY U vs FLOWRATE Q
U
(cm/sec)
x T-piece inlet
▲ Ring inlet, injection in branch
o Ring inlet, injection in straight run
Equation to best least squares straight line U = 1,694Q
5,0
5,5
5,0
4,5
4,0
3,5
3,1
2,5
2,0
1,5
1,0
0,5
0
0
0,5
1,0
1,5
2,0
2,5
3,0
3,5
Q (litres/min)

FIGURE 6.2

AXIAL DIFFUSION COEFFICIENT D_a vs FLOWRATE Q

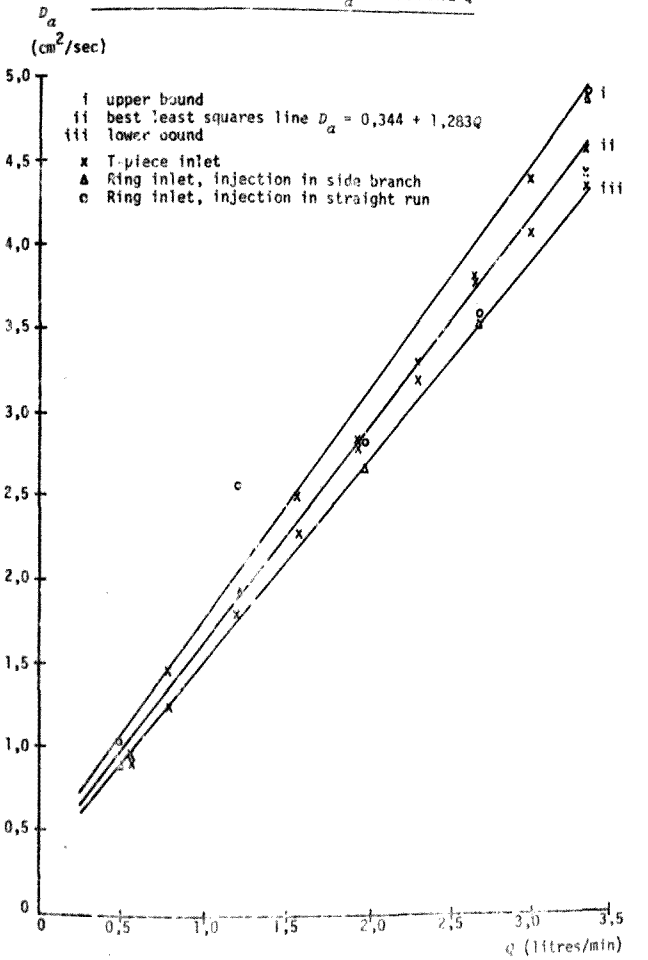

FIGURE 6.3

FIGURE 6.4

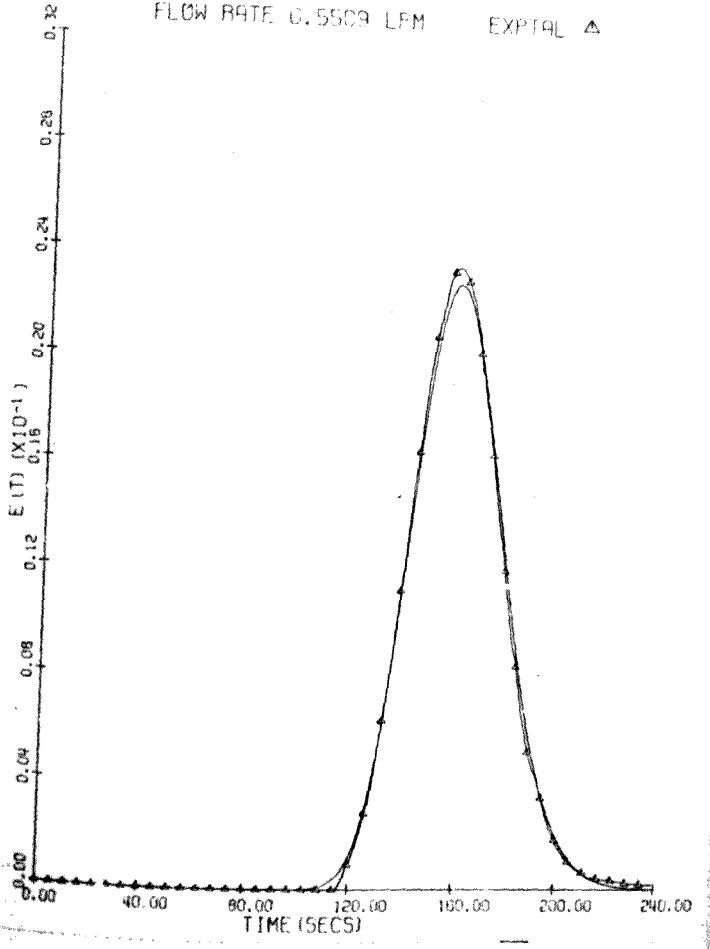
RUN NO. 1
FLOW RATE 0.5509 LPM
EXPTAL △
E(T) (X10-1)
0.00
0.04
0.08
0.12
0.16
0.20
0.24
0.28
0.32
0.00
40.00
80.00
120.00
160.00
200.00
240.00
TIME (SECS)

FIGURE 6.5

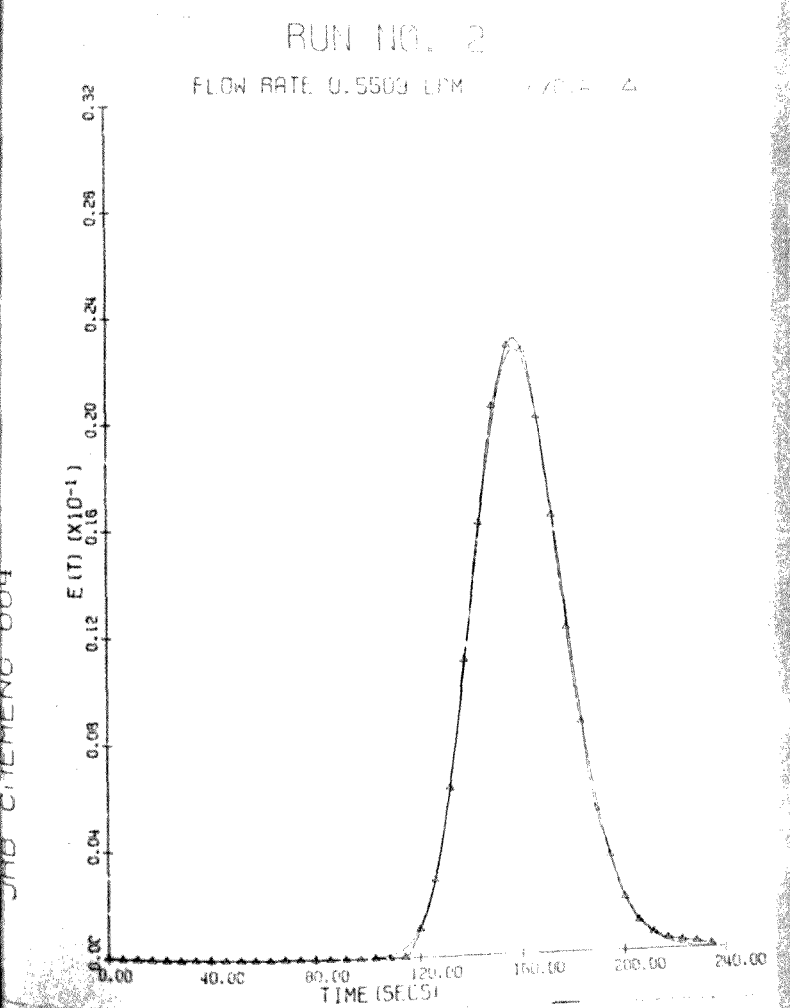
RUN NO. 2
FLOW RATE 0.5500 LPM
E(T) (X10⁻¹)
0.00
0.04
0.08
0.12
0.16
0.20
0.24
0.28
0.32
0.00
40.00
80.00
120.00
160.00
200.00
240.00
TIME (SECS)

FIGURE 6.6

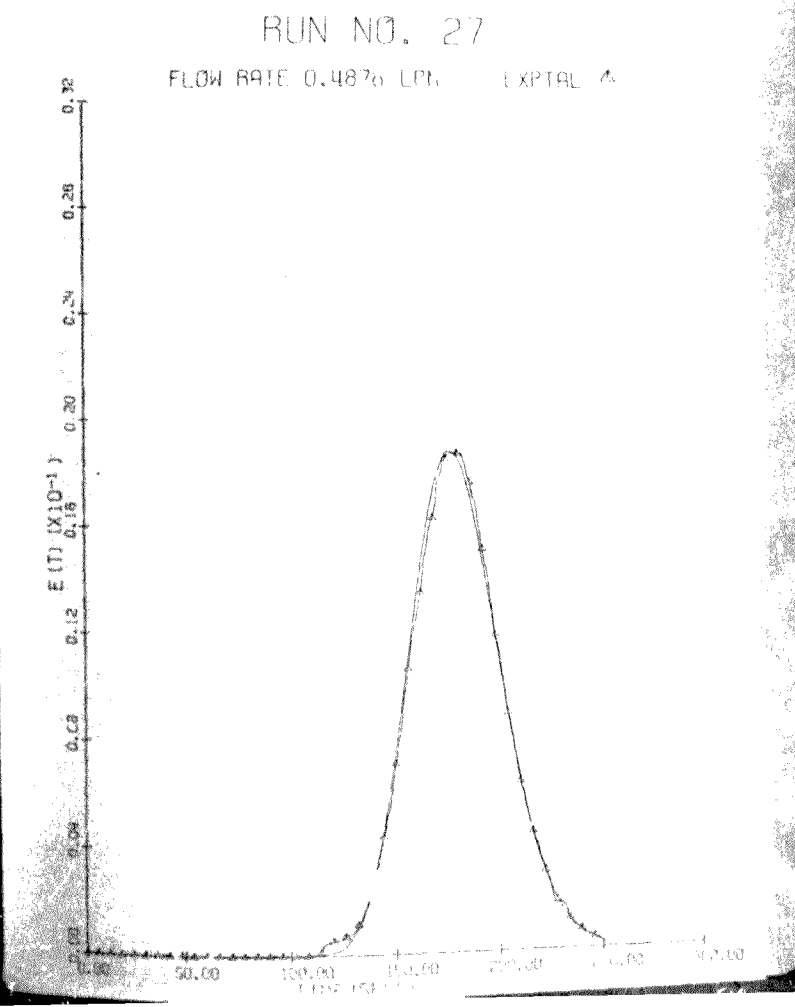
RUN NO. 27
FLOW RATE 0.487 LPM
EXPTAL
E(T) (X10⁻¹)
0.32
0.28
0.24
0.20
0.16
0.12
0.08
0.04
0.00
50.00
100.00
150.00
200.00
250.00
300.00

FIGURE 6.7

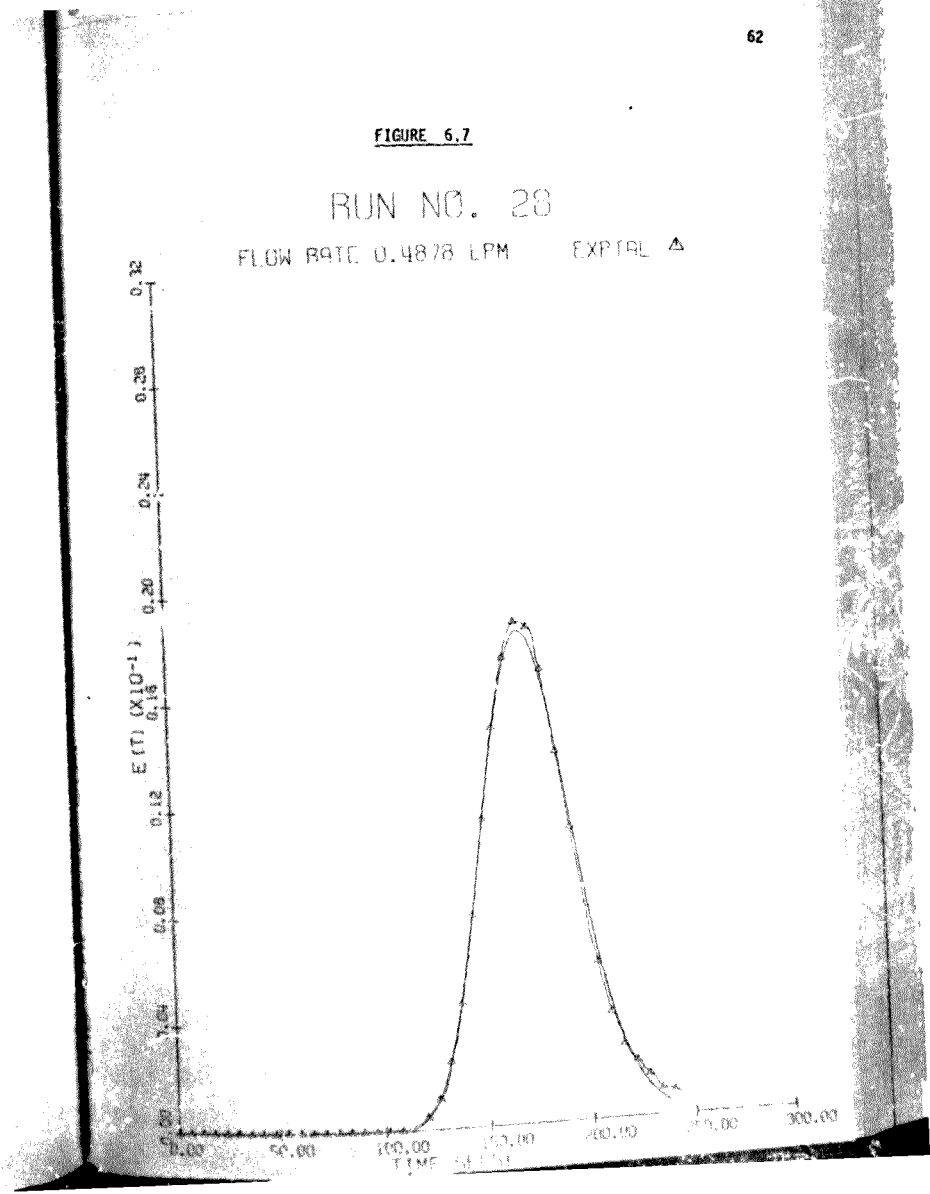
RUN NO. 28
FLOW RATE 0.4878 LPM
EXPTRL
E(T) (X10⁻¹)
0.32
0.28
0.24
0.20
0.16
0.12
0.08
0.04
0.00
50.00
100.00
200.00
300.00
TIME

FIGURE 6.8

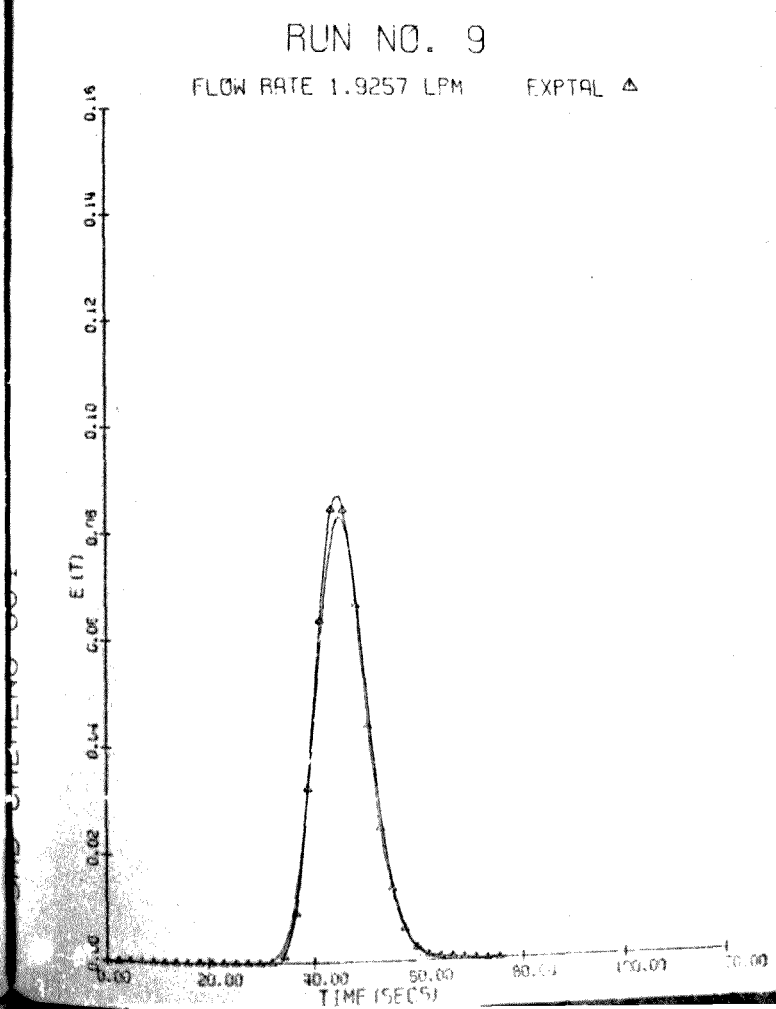
RUN NO. 9
FLOW RATE 1.9257 LPM
EXPTAL Δ
E(T)
0.16
0.14
0.12
0.10
0.08
0.06
0.04
0.02
0.00
0.00
20.00
40.00
60.00
80.00
100.00
120.00
TIME (SECS)

FIGURE 6.9

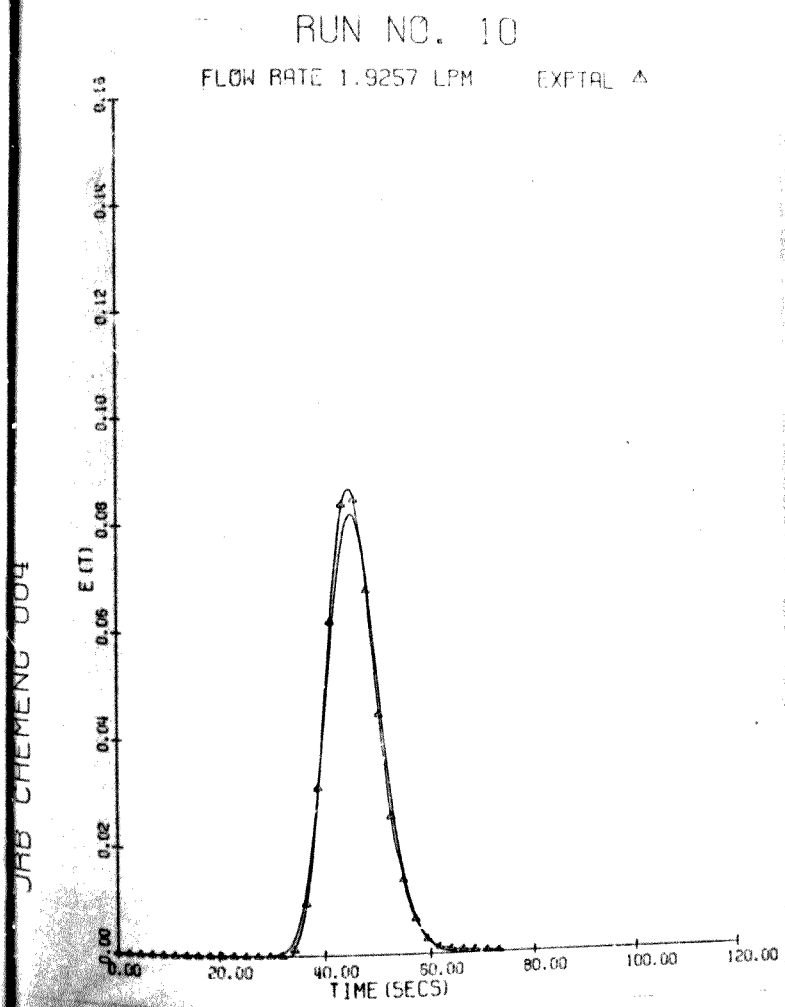

FIGURE 6.10

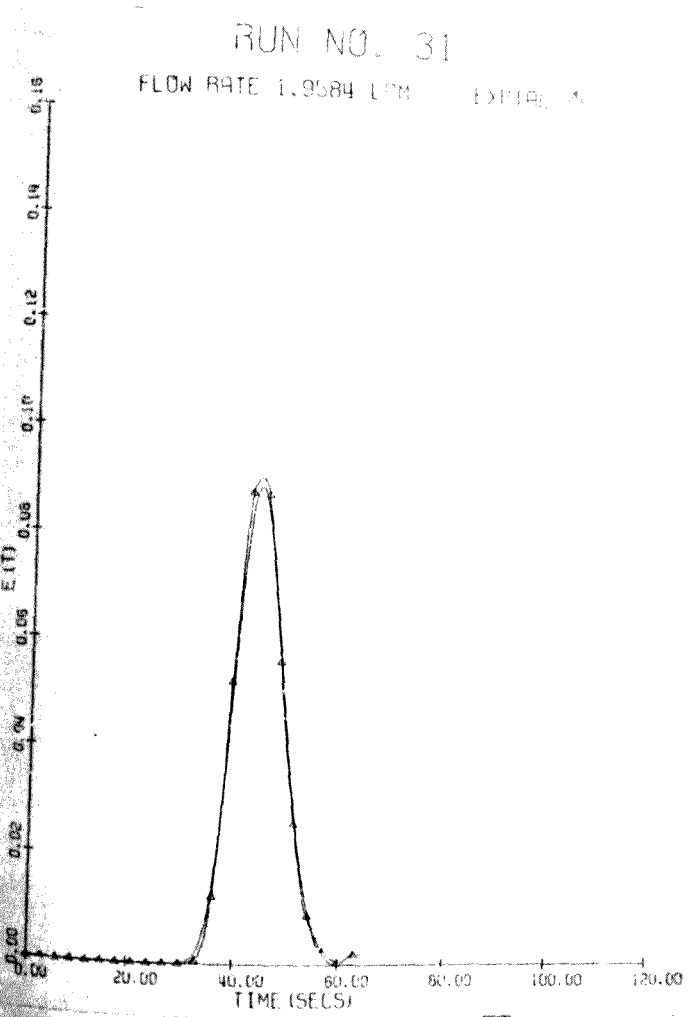
RUN NO. 31
FLOW RATE 1.9584 LPM
E(T)
0.00
0.02
0.04
0.06
0.08
0.10
0.12
0.14
0.16
0.00
20.00
40.00
60.00
80.00
100.00
120.00
TIME (SECS)

FIGURE 6.11

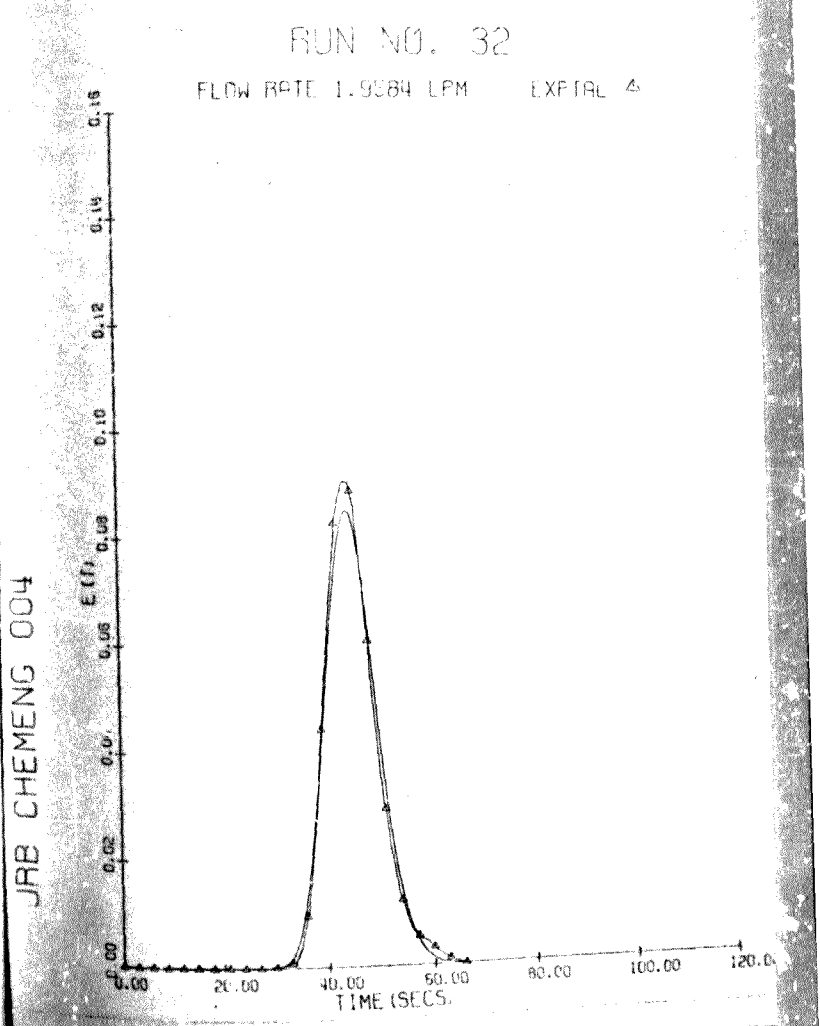
RUN NO. 32
FLOW RATE 1.9584 LPM
EXPTAL 4
E(T)
0.16
0.14
0.12
0.10
0.08
0.06
0.04
0.02
0.00
0.00
20.00
40.00
60.00
80.00
100.00
120.0
TIME (SECS.
JRB CHEMENG 004

FIGURE 6.12

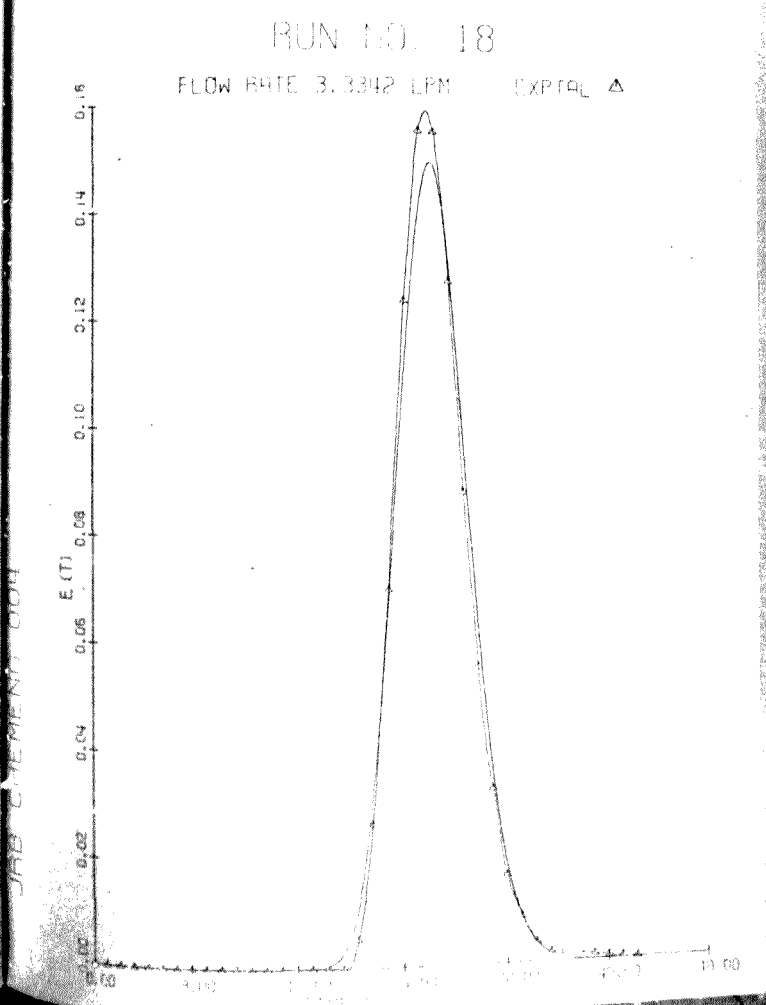
RUN NO. 18
FLOW RATE 3.3342 LPM
EXPTAL Δ
E(T)
0.16
0.14
0.12
0.10
0.08
0.06
0.04
0.02
0.00
0.00

FIGURE 6.13

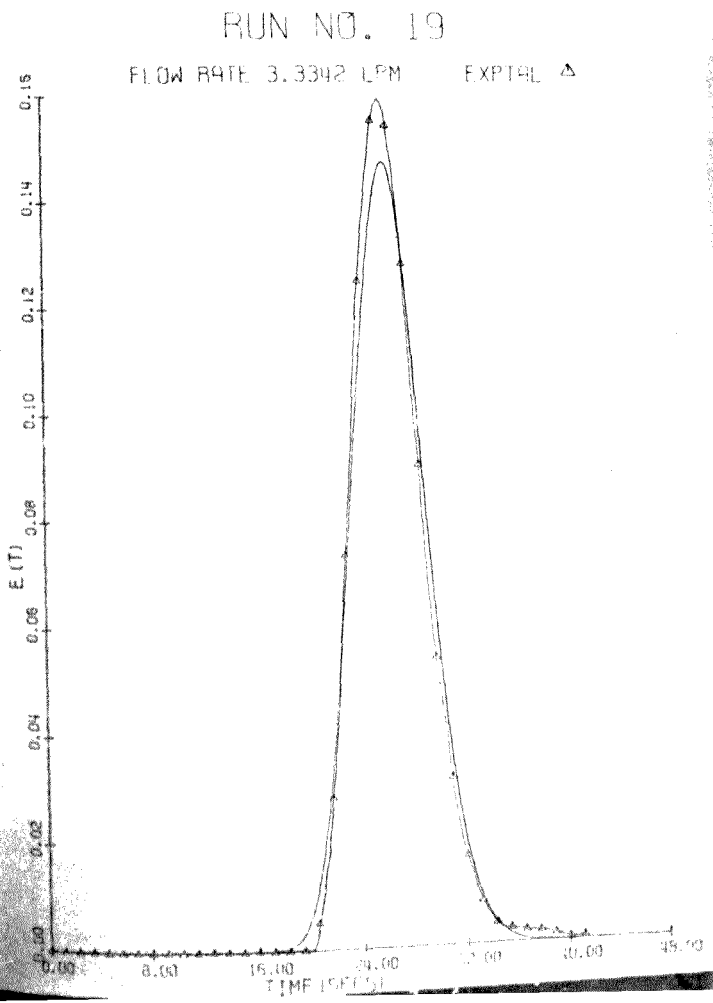
RUN NO. 19
FLOW RATE 3.3342 LPM
EXPTAL
E(T)
0.00
0.02
0.04
0.06
0.08
0.10
0.12
0.14
0.16
0.00
8.00
16.00
24.00
30.00
45.00
TIME (SEC)

FIGURE 6.14

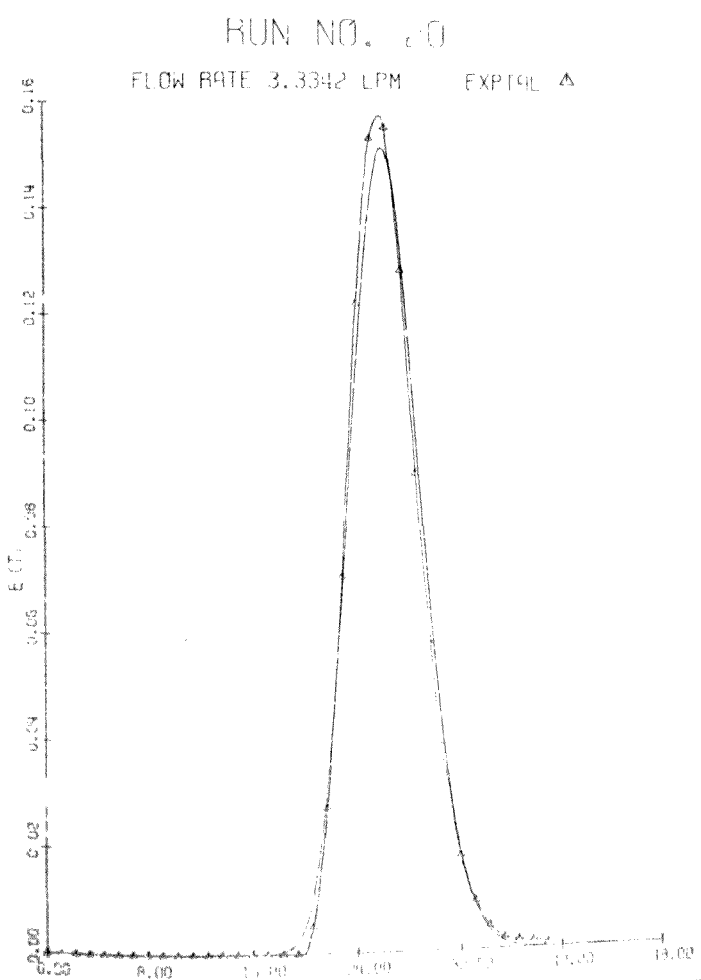
RUN NO. 20
FLOW RATE 3.3342 LPM
EXPT9L A
E(T)
0.16
0.14
0.12
0.10
0.08
0.06
0.04
0.02
0.00
0.00
4.00
8.00
12.00
16.00

FIGURE 6.15

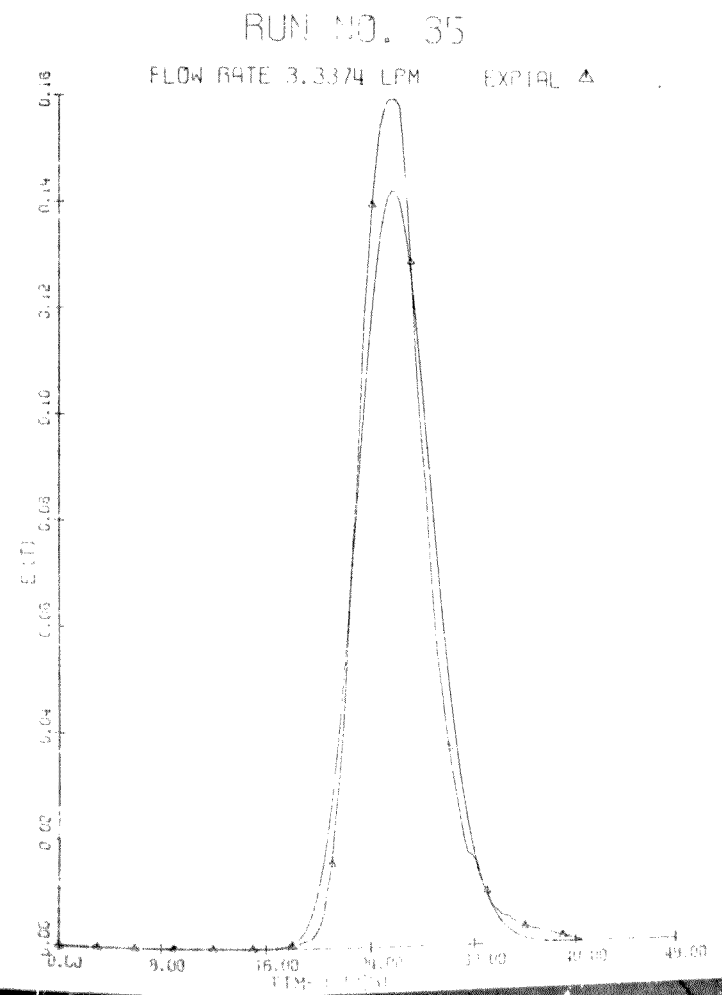
RUN NO. 35
FLOW RATE 3.3374 LPM
EXPTAL Δ
E(T)
0.16
0.14
0.12
0.10
0.08
0.06
0.04
0.02
0.00
0.00
8.00
16.00
24.00
32.00
40.00
48.00

FIGURE 6.16

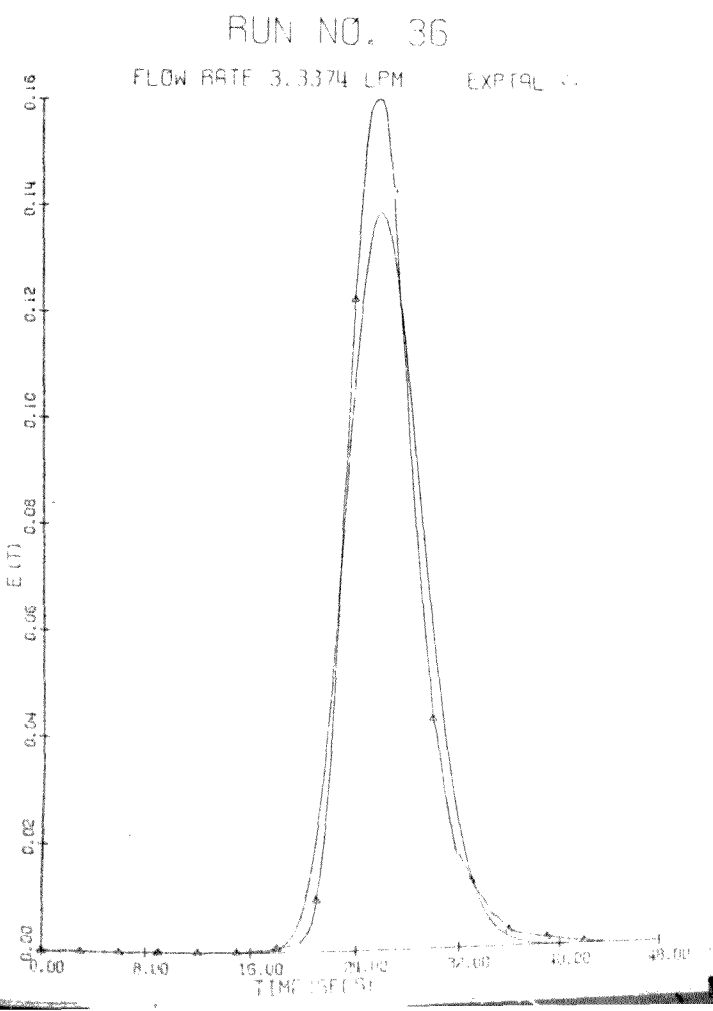
RUN NO. 36
FLOW RATE 3.3374 LPM
E(T)
0.00
0.02
0.04
0.06
0.08
0.10
0.12
0.14
0.16
0.00
8.00
16.00
24.00
32.00
40.00
48.00
TIME (SEC)

and the holdup volume in the column was not affected when the column was repacked.

On the other hand, the high variance of estimate obtained for the D_a data shows that the mathematical model is not sensitive to this parameter. This agrees with the findings of other workers (see 3.4.2.a).

In order to test the sensitivity of the axial dispersion model to D_a, two straight lines (i) and (iii) were drawn on Figure 6.3, representing roughly the upper and lower bounds of the data. Values of D_a obtained from each line were used to solve the reaction plus diffusion equation 3.14 for a range of flowrates. The results are given in Table 9.1, and show that no appreciable difference was made to the reactor concentration profile by choice of D_a values from either (i) or (iii). The best least squares straight line (ii) was thus used to obtain values of D_a for comparison with other models.

From Figures 6.4-6.16 it will be seen that in all cases the theoretical curve rises less steeply than the experimental initially, has a lower turning point, and falls less steeply than the experimental curve. Further, as the flowrate becomes greater, the fit between experimental and theoretical curves worsens - this is due to the fact that the pulse injection time is no longer negligible compared to reactor residence time at high flow rates.

It can be seen that the runs at any flowrate are indistinguishable from one another, except that those for runs 28, 31, 35 and 36 give a poor fit due to baseline drift on the recorder trace, and poor recorder response toward the end of the curve.

5.6 HOLDUP VOLUME

Using a column length of 149,8 cm., plus the values of Q

and U from Table 6.1, a value of column holdup volume could be obtained at each point from:-

$$V_h = \frac{149,8\ Q}{80\ U} \qquad 6.3$$

V_h = column holdup volume (litres)

Q = volumetric flowrate (litres/min.)

U = velcoity (cm./sec.)

The mean value of the holdup was 1,472 litres, with a standard deviation of 0,011.

The holdup volume obtained by weighing (see Appendix v) was 1,43 litres, which differs from the above by 2,8%. However, as discussed in Appendix v, the accuracy of this latter value is suspect. Note that both methods of calculating holdup volume took the inlet and outlet tubing volumes into account. For determination of holdup volume for short column see Appendix v.

6.7 CONCLUSIONS

The one point tracer injection technique used in this work to obtain an $E(t)$ curve together with characterisation of this curve by its mean and variance, yielded reproducible values of U and D_a which gave excellent fit between experiment and theory. The skewness of the curve cannot be used either to obtain, or to check, U and D_a values.

Use of the $E(t)$ curve and U and D_a to solve the equations for reaction plus diffusion is discussed in 3.4.2.e.

CHAPTER 7

7.1 EXPERIMENTAL PROCEDURE

A flowsheet for the reactor is given in Figure 5.2. In order to obtain the same inlet concentration of reactants at different flowrates, it was necessary to keep the flowrates of the two inlet streams in a constant ratio to one another. Identical flowmeters were used for both these streams, so the meter readings were set equal at each flowrate. This ensured that:-

$$\frac{Q_1}{Q_2} = 1$$

and consequently that

$$Q_3 = 2Q_1 = 2Q_2 \qquad (7.1)$$

It can thus be seen that the stock streams were diluted 50% on entering the reactor. This meant that the stock concentrations of diacetate and caustic had to be double the inlet concentrations.

In order to calculate the required acetic acid quench stream concentration for any run, the procedure was as follows. Using the inlet concentrations for the run, the plug flow model for the reactor was solved to obtain the maximum and minimum expected caustic concentrations in the outlet, corresponding to the maximum and minimum possible inlet rotameter settings. The upper and lower limits of the quench stream rotameter were also known, and a quench stream concentration could thus be obtained which would be sufficiently high to neutralise the outlet stream at the maximum flow rate, and sufficiently low to do likewise at the minimum flowrate.

The inlet and quench solutions were made up in the stock tanks using distilled water. Some time before the commencement of the run, the stock tanks were filled and the stirrers and heaters

and temperature controllers all switched on. The acetic acid, caustic soda and diacetate were then weighed in. While the stock solutions were heating up, the reactor system was checked for leaks and air bubbles, and all ancillary equipment such as pH meters, balances and nitrogen bleeds was made ready.

When the stock solutions reached the desired temperatures, each was allowed to run to waste for one minute (roughly twice the residence times in the inlet flow lines) to clear the water out of the lines, and sampled into a 750 cm^3 flask. The flasks were fitted with rubber stoppers wrapped in aluminium foil, and the caustic soda solution was sampled and stored under nitrogen.

The rotameters were calibrated from 10-100% of the full flow, but the usable range of readings was 20-90, so the meter settings used were approximately 20, 30, 50, 70 and 90 for each run. This meant that most runs gave five points on the concentration-residence time curve for the reactor. For some of the runs intermediate settings were used as well.

Both inlet streams were thus set at each of the readings in turn, and the quench stream was adjusted until the pH of the quenched outlet was at the desired value. Once the desired pH was reached the streams were allowed to flow undisturbed for roughly twice the residence time at that flowrate, to ensure that the reactor was truly at steady state. The reactor inlet and outlet temperatures were then recorded, together with the readings on all three rotameters. The pH of the quenched solution was also recorded, and a 750 cm^3 sample was taken of the quenched stream. This sample was also collected and stored under nitrogen.

For some of the experiments only inlet stream samples were taken and analysed, and only the outlet concentration of the caustic

soda was calculated. (See Appendix ix).

At the end of the run the three streams were sampled again to check if there had been any change in stock concentration during the run, and then each of the rotameters was calibrated in turn at the readings obtained during the experiment.

(Rotameter calibration and pH meter standardisation and choice of neutralisation end points are all discussed in the appendices.)

The samples collected during the run were then analysed for sodium hydroxide, acetic acid, diacetate, monoacetate and glycol as discussed in section 8.4, and all necessary densities were measured, as in Appendix ii.

The flowrates and titration volumes obtained during the experiments were used as the input to a computer program which calculated the experimental residence time and inlet and outlet concentrations, and compared the results to those predicted by the plug flow model.

7.2 REACTION EXPERIMENTS

A total of thirteen runs was carried out, using a range of inlet temperatures and concentrations, and both the T-piece and ring inlets. These runs and the results are summarised in Appendix ix and discussed in Chapter 9.

CHAPTER 3

8.1 INTRODUCTION

It was found that the flowmeters used in this work could be calibrated with an accuracy of 99%. It was decided that this level of accuracy would be maintained for all other measurements in this work.

A reactor system flow sheet showing all streams and concentrations is given in Figure 5.2. Since the lines for streams 3 and 4 were left as short as possible to reduce reaction in them, these streams could not be sampled directly. Reactor inlet and outlet concentrations therefore had to be calculated from mole balances based on analysis of streams 1, 2, 5 and 6.

Streams 2 and 5 could obviously be analysed by simple acid-base titrations, and the techniques used are given below. Since the amount of sodium acetate formed in the reactor is equal to the caustic soda reacted, no attempt was made to measure the former.

Analysis of streams 1 and 6 was more difficult, however, due to the problems involved in analysing for the diacetate, monoacetate and glycol in the same solution.

8.2 INFRARED SPECTROSCOPY

A Beckman IR5A infrared spectrophotometer was used to obtain spectra of pure diacetate, pure glycol, and a mixture of mono- and diacetate and glycol. The spectra of the diacetate, monoacetate and glycol were too similar to enable the spectroscope to be used to measure these substances quantitatively

8.3 GAS CHROMATOGRAPHY

It was found that water, acetic acid, diacetate, monoacet-

ate and glycol could be separated on a 50 cm. column of "Porapak" Q" 80-100 mesh. (Waters Association Inc. Framingham, Mass. U.S.A.). The separation was carried out on a Perkin Elmer F6 Fraktometer at a column temperature of 200°C using helium as a carrier gas. The total time for the separation was 15 minutes at a carrier gas pressure of 30 psi, and flow rates of carrier and reference streams of 1,7 cm^3/second. At lower temperatures and pressures the diacetate peak, which was the last to appear, tended to "tail" rather badly. Unfortunately the upper limit of temperature for Porapak is 200°C, and slow degradation of the packing took place causing baseline drift on the detecting instruments.

The Fraktometer has both a hot wire conductivity meter and a flame ionisation detector. It was found that the hot wire output was non-linear with concentration for the substances being analysed, and calibration would have been difficult, since pure monoacetate was unobtainable. Although the flame ionisation detector output is linear with concentration, it was found to be very difficult to keep the flow of oxygen and hydrogen to this instrument constant.

Another problem arose when the quenched reaction mixture was analysed. This contained sodium acetate which caked the interior of the chromatograph when the sample was vaporised.

Finally, when difficulty was experienced in injecting a reproducible sample volume into the chromatograph, it was decided that analysis by gas chromatograph would be abandoned.

8.4 ANALYSIS BY WET CHEMISTRY

Since it had already been decided to analyse streams 2 and 5 by acid-base titrations, it was felt that the techniques involved could possibly be extended to cover complete analysis of all streams.

The acetic acid present in stream 1 could, of course, be analysed by titration as for stream 5. The total acetate present in any stream could be measured by saponifying to completion with standard alkali and backtitrating with standard acid (Siggia (1958) pages 46-47).

It will be shown later (in Appendix vi) that if ethylene glycol can be analysed independently of the other components in a stream, then it will be possible to obtain the concentration of each component in the stream. A method for glycol analysis was therefore sought.

Malaprade (1926, 1928, 1934) discovered that molecules containing hydroxyl groups attached to adjacent carbon atoms are readily oxidised by periodic acid, the periodic acid being reduced to iodic acid in the process. The discovery was confirmed by Fleury and Lange (1933), Fleury, Herissey and Joly (1934), and Jackson and Hudson (1937).

Since ethylene glycol contains two such adjacent carbon atoms, the periodic acid oxidation provides a method for analysing this substance in the presence of mono- and diacetate, since the latter would be unaffected by the oxidation.

Siggia (1958) pages 16-18, gives a method of analysis for dihydroxy compounds in aqueous solution. This method is based on that of Pohie, Mehlenbacher and Cook (1945), and is as follows for glycol:-

The glycol is oxidised with periodic acid in a 14N acetic acid solution. The reaction proceeds as follows:-

$$\begin{matrix} CH_2OH \\ | \\ CH_2OH \end{matrix} + HIO_4 \xrightarrow[HAc]{14N} 2\,HCHO + H_2O + HIO_3$$

glycol — periodic acid — formaldehyde — iodic acid

When the oxidation is complete, potassium iodide is added to liberate iodine from the periodic and iodic acids:-

$$HIO_4 + 7KI + 7HAc \longrightarrow 7KAc + 4I_2 + 4H_2O \qquad II$$

$$HIO_3 + 5KI + 5HAc \longrightarrow 5KAc + 3I_2 + 3H_2O \qquad III$$

The liberated iodine can then be titrated with sodium thiosulphate. A blank is run on pure periodic acid and from the difference in the thiosulphate titrations between the pure and reduced acid, the glycol content of the original sample may be obtained.

There is a major difficulty involved in using this method for measuring glycol in the presence of its esters, and that is that the saponification reactions are catalysed by acids. Hence while the above oxidation is taking place, side reactions will be forming more glycol as follows:-

$$\begin{matrix} CH_2COOCH_3 \\ | \\ CH_2COOCH_3 \end{matrix} + H_2O \xrightarrow{acid} \begin{matrix} CH_2OH \\ | \\ CH_2COOCH_3 \end{matrix} + CH_3COOH$$

diacetate — monoacetate — acetic acid

$$\begin{matrix} CH_2OH \\ | \\ CH_2COOCH_3 \end{matrix} + H_2O \xrightarrow{acid} \begin{matrix} CH_2OH \\ | \\ CH_2OH \end{matrix} + CH_3COOH$$

monoacetate — glycol — acetic acid

When tested on standard glycol solutions containing varying amounts of mono- and diacetate, it was found that the glycol concentrations could be in error up to 10%, which is well outside the error limit of 1% set for this work.

An investigation was then carried out to determine whether the acid concentration of the oxidising solution could be reduced and the saponification reaction thus slowed down to an acceptable

level.

Hess, Jordan and Ross (1956), give a method for the rapid quantitative determination of glycol in water, in which the oxidation takes place in approximately 0,6 N nitric acid. Further, Allen, Charbonnier and Coleman (1940) in their method for the quantitative determination of certain polyalcohols in the presence of each other used pure periodic acid as their oxidising agent.

Price and Kroll (1938, 1942) have studied the kinetics of the periodate oxidation of 1,2 glycols. They found that in the pH range 7,5-10, the rate constant for the oxidation of glycol was dependent on pH, but from pH 2-7,5 the rate was independent of pH.

On the basis of the above, it was decided that periodic acid alone would be used to oxidise the ethylene glycol, and that other acids would not be added. It was hoped that the periodic acid would not catalyse the saponification to any great extent since it is a weak acid.

Since an acid medium is required for the iodine liberation reactions II and III, it was decided that, to minimise acid saponification, this acid would be pipetted into the oxidising mixture just after adding the potassium iodide.

For both the acid-base and iodine titrations, a Radiometer pH meter was used, coupled to an automatic titrating device which operated a solenoid valve. It was felt that the analysis could be done quicker and more accurately with these instruments than by hand. All analysis was done by weight rather than by volume, since once again the weighing could be done quicker and more accurately. The complete analysis procedure, and details of the analytical apparatus used, and the determination of the titration endpoints are discussed in Appendix vi. Density determinations are given in Appendix ii.

8.5 ERROR GROWTH DURING ANALYSIS

As explained in Appendix vi, all analyses were repeated until at least four were obtained which agreed to within 99%. Unfortunately, however, the insensitivity of the glycol analysis (Appendix vi - 2) plus the fact that certain concentrations were obtained by subtraction from other concentrations, led to a disproportionate growth of errors during the analysis. Consider for example the following case:-

A diacetate feed stream with diacetate X_{1s} molar and monoacetate X_{3s} molar is to be analysed. Following the procedure outlined in Appendix vi, section 1:-

$$X_{1s} + X_{3s} = \frac{u\rho_1}{2l\rho_{10}}\left(\frac{wm}{v} - s\right) \qquad 13$$

where u = molarity of standard thiosulphate

ρ_1 = sample density

ρ_{10} = thiosulphate density

l = sample weight

w = grams of u molar thiosulphate used to titrate periodic acid blank

s = grams of u molar thiosulphate used to titrate periodic acid in samp'

v = grams of periodic acid taken for blank.

Now assume that the following values were obtained during analysis:-

Total acetate = 0,206M

u = 0,1M

ρ_1/ρ_{10} = 1,0

l = 20 gm.

w/v = 5

m = 40 gm.

s 157,6 gm.

Hence, total glycol $= X_{1s} + X_{3s} = \frac{0,1}{40}(200 - 157,6) = 0,106M$

Total acetate $= 2X_{1s} + X_{3s} = 0,206$

Hence $X_{1s} = 0,206 - 0,106 = 0,1M$

and $X_{3s} = 0,106 - 0,1 = 0,006M$

If w/v is now increased by 1%, all other values remaining constant,

$$\frac{w}{v} = 5,05$$

Hence $X_{1s} + X_{3s} = \frac{0,1}{40}(202 - 157,6) = 0,111M$

$X_{1s} = 0,206 - 0,111 = 0,095M$

$X_{3s} = 0,111 - 0,095 = 0,016M$

Hence a 1% error in w/v causes a 5% difference in X_{1s} and a 267% difference in X_{3s}. These errors, of course, become compounded when w/v is used for several glycol concentration measurements.

In order to study this effect for changes in other standard concentrations and densities and flowrates, a computer program was written to increase each of these in turn by 1% and to print out the resulting variations in reactor system concentrations. Tables 8.1 - 8.3 give the results for a typical set of stock, inlet and outlet concentrations respectively. In each table the first line represents the values obtained with no errors in the parameters, and each successive line represents values for a 1% increase in the parameter in the left hand column. A blank in the table indicates that this particular concentration was unaffected by the variation in the parameter. For the meanings of all parameters see the nomenclature section.

From Table 8.3 the following maximum percentage errors can be obtained in outlet concentrations for a 1% change in any one parameter:-

TABLE 8.1

STOCK STREAMS SENSITIVITY ANALYSIS

Parameter varied by 1%	X_{1s}	X_{3s}	X_{2s}	X_{6s}
	0,09308	0,00139	0,1950	0,1101
c	0,09698	-0,00252	-	0,1112
d	0,09118	0,00328	-	-
e	0,09698	-0,00252	-	-
h	0,09102	0,00343	-	-
j	0,09104	0,00342	0,1970	-
l	0,09405	-0,00058	-	-
u	0,09213	0,00330	-	-
w/v	0,08831	0,01090	-	-
x	-	-	0,1931	-
y	-	-	0,1970	-
α	-	-	-	0,1090
β	-	-	-	0,1112
ρ_1	0,09401	0,00140	-	-
ρ_3	-	-	0,1970	-
ρ_5	-	-	-	0,1112
ρ_7	0,08917	0,00529	-	0,109
ρ_8	0,09510	-0,00065	0,1931	-

TABLE 8.2

INLET REACTOR STREAM SENSITIVITY ANALYSIS

Parameter varied by 1%	X_{1o}	X_{2o}	X_{3o}
	0,04755	0,09541	0,00071
a	0,04954	-	-0,00129
d	0,04658	-	0,00168
e	0,04954	-	-0,00129
G_1	0,04780	0,09492	0,00066
G_2	0,04733	0,09590	0,00066
h	0,04650	-	0,00176
j	0,04651	0,09636	0,00175
l	0,04805	-	-0,00030
u	0,04706	-	0,00168
w/v	0,04512	-	0,00557
x	-	0,09446	0,00066
y	-	0,09636	0,00066
ρ_1	0,04779	0,09589	-
ρ_2	0,04780	0,09587	0,00066
ρ_7	0,04555	-	0,00270
ρ_8	0,04858	0,09445	-0,00033

TABLE 8.3

OUTLET REACTOR STREAM SENSITIVITY ANALYSIS

Parameter varied by 1%	x_{1f}	x_{2f}	x_{3f}	x_{5f}
	0,00572	0,02693	0,01447	0,02807
c	0,01198	0,02720	0,00821	-
d	0,00282	-	0,01737	-
e	0,01171	-	0,00848	-
g_1	0,00636	0,02679	0,01410	0,02801
g_2	0,00494	0,02680	0,01504	0,02801
g_5	0,00614	0,02720	0,01400	0,02809
h	0,00258	-	0,01761	-
j	0,00165	-	0,01854	-
l	0,00820	-	0,01152	0,02804
l'	0,00581	-	0,01438	0,02804
l''	0,00552	-	0,01494	0,02776
u	0,00357	-	0,01583	0,02835
w/v	-0,00342	-	0,02303	0,03108
x	0,00676	-	0,01344	0,02803
y	0,00485	-	0,01535	0,02803
α	0,00555	0,02666	0,01465	0,02803
β	0,00608	0,02720	0,01411	0,02803
ρ_1	0,00575	0,02707	0,01454	0,02821
ρ_2	0,00584	0,02706	0,01445	0,02817
ρ_5	0,00581	-	0,01438	0,02803
ρ_7	-0,00054	0,02666	0,02072	-
ρ_8	0,00979	-	0,01040	-

TABLE 8.4

X_{1f}	X_{2f}	X_{3f}	X_{5f}
+83,5%	+1%	+47,6%	+10,2%
-228%	-1%	-57,0%	-1,11%

Several points emerge from this analysis:-

(i) Since the outlet concentration of caustic soda, X_2, is the most accurate, this should be used for testing the various reactor models

(ii) The ratio w/v is critical, and great care must be taken to obtain an accurate value for this quantity (in practice this quantity was measured until 8 values were found which differed by not more than 1%, and the mean of these values was used.)

(iii) The values in Table 8.4 above represent the minimum expected differences between experimental and theoretical outlet concentrations. If more than one parameter varies by up to 1%, and if inlet concentrations vary too, the errors could be considerably greater.

CHAPTER 9

9.1 RESULTS

The computer solutions of the mathematical model equations are presented first, followed by the experimental results obtained on the packed bed reactor.

9.1.1 Results from Mathematical Models

In order to afford a comparison between the performance of the CSTR and the ideal TFR, equations 3.4 (batch/ideal TFR) and equation 3.8 (CSTR) were solved to give monoacetate concentration, X_g, as a function of residence times, τ, in these reactors. The inlet concentrations and temperatures used, together with the resulting concentration-residence time profiles, are given in Figures 9.1 and 9.2. By comparison with 5.1.2 it will be seen that the inlet concentrations used for these profiles lay within the range of reactor operating conditions chosen for this work. These figures also show that at low reaction temperatures, higher maximum concentrations of monoacetate are obtained than at high temperatures, as predicted in section 4.3.

The ideal TFR equations were also solved to give the predicted outlet concentration from the reactor corresponding to each set of experimental inlet concentrations and residence times. The results of these computations are given in Appendix ix, where they are compared to the outlet concentrations obtained experimentally.

In section 6.5 it was decided that, in order to test the sensitivity of the axial dispersion model to the axial diffusion coefficient, D_a, equations 3.14 would be solved using values of D_a from curves (i) and (iii) on Figure 6.3. Profiles were obtained for a fixed set of inlet concentrations, and a range of flowrates. The profiles which showed the greatest divergence were those at low flow

rates, an example of which is given in Table 9.1. It can be seen from this table that the choice of D_a in the given range does not affect the profiles. Values of D_a used for comparing the axial dispersion model to the other models were thus taken from curve (ii) Figure 6.3, which is the best least squares straight line through all the D_a data.

As discussed in 3.4.2.f the segregated flow model could be solved by using either an experimental or calculated residence time distribution function. In addition, several experimental distributions were obtained at each flowrate. Table 9.2 shows the outlet concentrations predicted by experimental and calculated distribution functions obtained at the same flowrate for five different runs compared to that predicted by the plug flow model. Table 9. shows similar predicted concentrations for a range of flowrates.

Figures 9.3-9.6 show the axial dispersion and plug flow model concentration profiles for a fixed set of inlet concentrations and varying flowrates. The experimental outlet concentrations obtained for these inlet concentrations are also given for comparison.

9.1.2 Results of Experiments on Packed Reactor

Thirteen runs were carried out in all, ten with the T-piece inlet, and three with the ring inlet. These runs yielded 99 experimental outlet concentrations for the reactor, of which 46 gave a complete outlet stream analysis, and 53 only the caustic concentration in the outlet.

The inlet and outlet concentrations obtained, together with the run temperatures and residence times and reactor volumes are given in Appendix ix.

9.2 DISCUSSION OF RESULTS

From Figures 9.1 and 9.2 it can be seen that in all cases

TABLE 9.1

CONCENTRATION PROFILES FOR VALUES OF D_a FROM CURVES (i) AND (iii), FIGURE 6.3

Temperature 26,0°C k_1 = 0,6017 litre/mole sec $D_a(i)$ = 2,33 cm^2/sec

v = 2,42 cm/sec k_2 = 0,2398 litre/mole sec $D_a(iii)$ = 1,99 cm^2/sec

Flowrate = 1,4262 litre/min

Reactor Length (cm)	X_1		X_2		X_3		X_5	
	(i)	(iii)	(i)	(iii)	(i)	(iii)	(i)	(iii)
0	0,04692	0,04692	0,09646	0,09646	0,00085	0,00085	0	0
7,486	0,03970	0,03968	0,08889	0,08887	0,00771	0,00774	0,00035	0,00035
14,975	0,03401	0,03397	0,08251	0,08248	0,01272	0,01277	0,00104	0,00103
22,464	0,02944	0,02939	0,07705	0,07701	0,01641	0,01647	0,00192	0,00192
29,953	0,02571	0,02566	0,07233	0,07228	0,01915	0,01920	0,00292	0,00291
37,443	0,02263	0,02258	0,06819	0,06815	0,02117	0,02122	0,00397	0,00397
44,932	0,02005	0,02000	0,06454	0,06449	0,02266	0,02271	0,00505	0,00505
52,421	0,01788	0,01784	0,06129	0,06124	0,02375	0,02380	0,00614	0,00614
59,910	0,01603	0,01599	0,05837	0,05833	0,02453	0,02458	0,00720	0,00720
67,400	0,01445	0,01441	0,05574	0,05570	0,02507	0,02511	0,00825	0,00825
74,889	0,01308	0,01304	0,05335	0,05331	0,02543	0,02546	0,00927	0,00927
82,378	0,01185	0,01185	0,05118	0,05113	0,02563	0,02568	0,01025	0,01025
89,867	0,01085	0,01081	0,04919	0,04914	0,02572	0,02576	0,01120	0,01121
97,356	0,00993	0,00989	0,04735	0,04731	0,02573	0,02575	0,01212	0,01212
104,846	0,00912	0,00909	0,04566	0,04562	0,02566	0,02568	0,01300	0,01300
112,335	0,00840	0,00837	0,04410	0,04406	0,02553	0,02555	0,01384	0,01385
119,824	0,00776	0,00773	0,04264	0,04260	0,02536	0,02538	0,01466	0,01467
127,313	0,00718	0,00715	0,04128	0,04125	0,02515	0,02517	0,01544	0,01545
134,803	0,00667	0,00664	0,04002	0,03998	0,02492	0,02493	0,01619	0,01620
142,292	0,00620	0,00618	0,03883	0,03880	0,02466	0,02468	0,01691	0,01692
149,781	0,00583	0,00580	0,03785	0,03780	0,02442	0,02443	0,01752	0,01754

TABLE 9.2

SEGREGATED FLOW MODEL

(i) Predicted outlet concentrations using experimental $E(t)$ function

(ii) Predicted outlet concentrations using calculated $E(t)$ function

Inlet concentrations:

X_{1o} = 0,04669 X_{2o} = 0,09694 X_{3o} = 0,00085 X_{5o} = 0

Flowrate: 3,3342 litre/min. Temperature: 27,0°C.

Run No.	X_{1f}		X_{2f}		X_{3f}		X_{5f}	
	(i)	(ii)	(i)	(ii)	(i)	(ii)	(i)	(ii)
18	0,01370	0,01369	0,05544	0,05540	0,02532	0,02530	0,00856	0,00855
19	0,01369	0,01369	0,05539	0,05539	0,02530	0,02530	0,00855	0,00855
20	0,01368	0,01368	0,05537	0,05538	0,02530	0,02530	0,00855	0,00856
35	0,01383	0,01387	0,05550	0,05570	0,02517	0,02524	0,00840	0,00843
36	0,01367	0,01366	0,05538	0,05533	0,02533	0,02529	0,00860	0,00858
Plug Flow model	0,01355		0,05520		0,02539		0,00860	

Note: There was a difference of two years between runs 18, 19 and 20, and runs 35 and 36, and different apparatus was used to take the measurements.

TABLE 9.3

SEGREGATED FLOW MODEL

(i) Predicted outlet concentrations using experimental $E(t)$ function

(ii) Predicted outlet concentrations using calculated $E(t)$ function

(iii) Plug flow predicted outlet concentrations

Inlet concentrations: X_{1o} = 0,2; X_{2o} = 0,4; X_{3o} = 0; X_{5o} = 0

Flowrates: Run no. 1 0,5509 litre/min. Run no. 10 1,9257 litre/min. Run no. 20 3,3342 litre/min.

Temperature: 25,0°C.

Run No.	X_{1f}			X_{2f}		
	(i)	(ii)	(iii)	(i)	(ii)	(iii)
1	0,00034	0,00034	0,00031	0,02587	0,02588	0,02554
10	0,00452	0,00453	0,00439	0,07471	0,07473	0,07417
20	0,01187	0,01187	0,01158	0,1116	0,1116	0,1108

Run No.	X_{3f}			X_{5f}		
	(i)	(ii)	(iii)	(i)	(ii)	(iii)
1	0,02520	0,02521	0,02491	0,1744	0,1744	0,1747
10	0,06567	0,06566	0,06539	0,1298	0,1298	0,1302
20	0,08789	0,08789	0,08768	0,1002	0,1002	0,1007

Inlet
concentrations: $X_{1o} = 0,01$ $X_{2o} = 0,02$

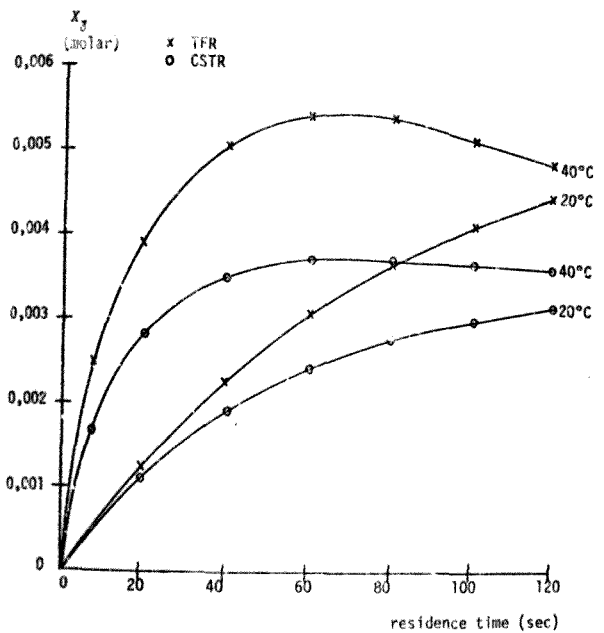

FIGURE 9.1

CSTR AND TFR CONCENTRATION PROFILES FOR MONOACETATE

Inlet concentrations: $X_{1o} = 0,1$ $X_{2o} = 0,2$

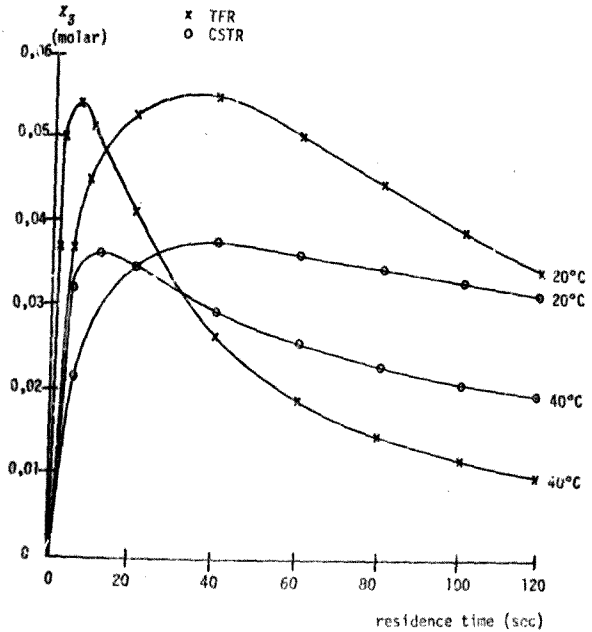

FIGURE 9.2

CSTR AND TFR CONCENTRATION PROFILES FOR MONOACETATE

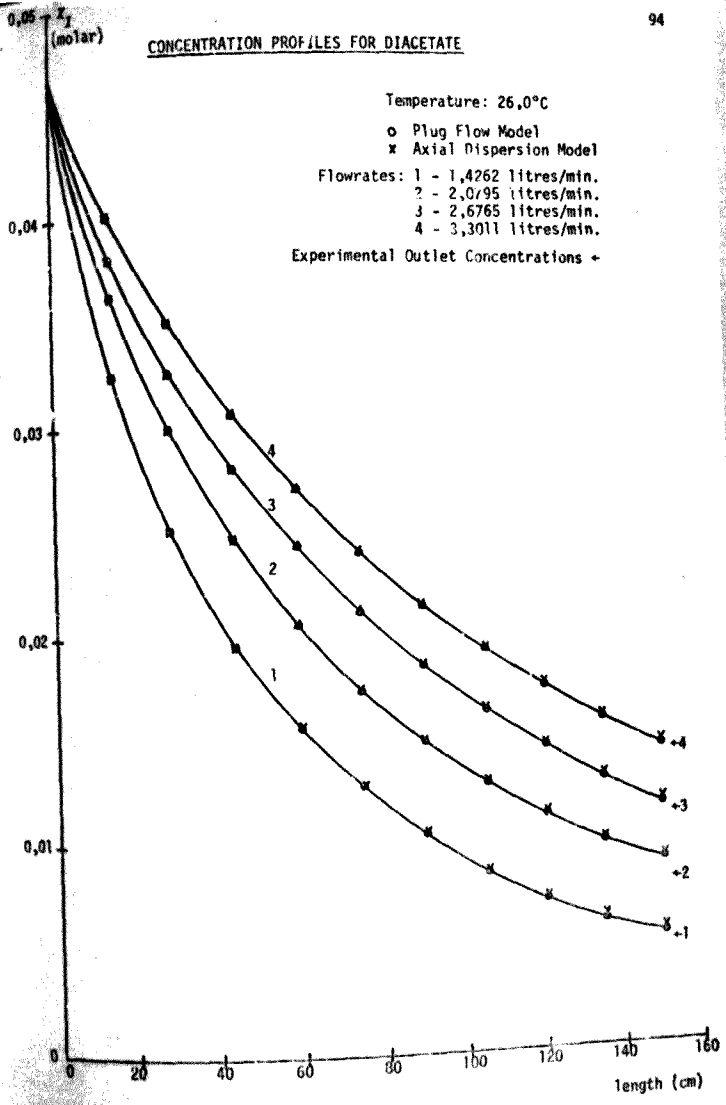
CONCENTRATION PROFILES FOR DIACETATE
Temperature: 26,0°C
o Plug Flow Model
x Axial Dispersion Model
Flowrates: 1 - 1,4262 litres/min.
2 - 2,0795 litres/min.
3 - 2,6765 litres/min.
4 - 3,3011 litres/min.
Experimental Outlet Concentrations ←
0,05 x_f (molar)
0,04
0,03
0,02
0,01
0
0
20
40
60
80
100
120
140
160
length (cm)
1
2
3
4
←1
←2
←3
←4

FIGURE 9.3

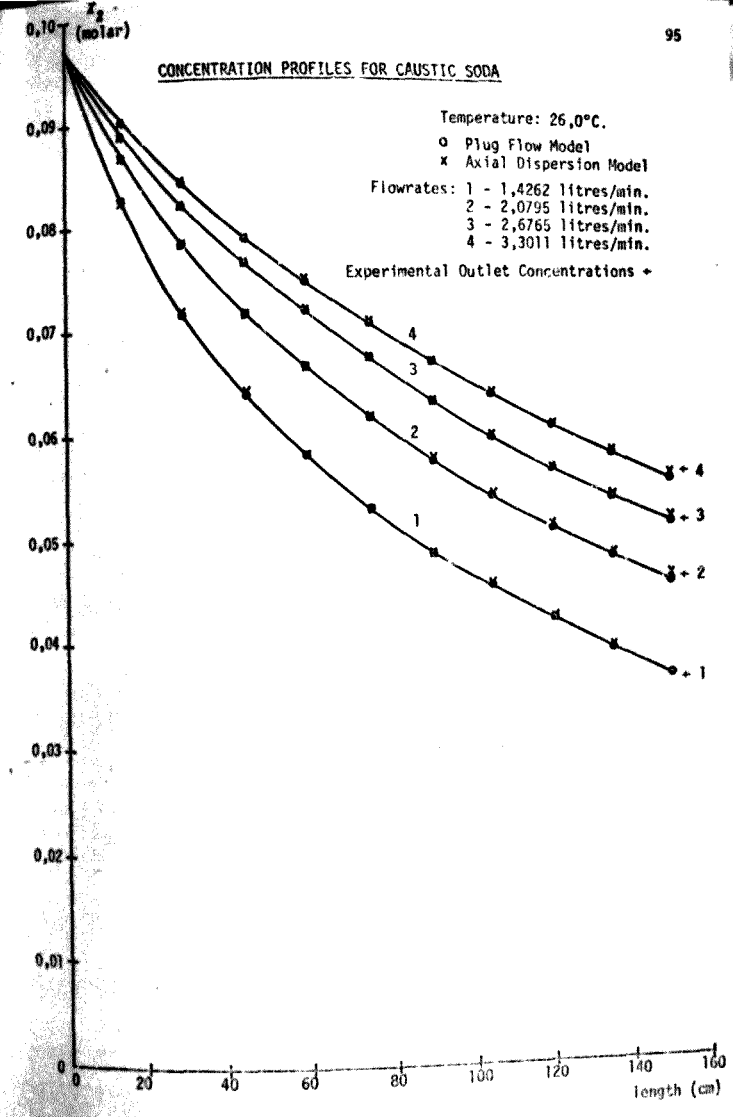
CONCENTRATION PROFILES FOR CAUSTIC SODA
$\bar{x}_2$ (molar)
Temperature: 26,0°C.
o Plug Flow Model
x Axial Dispersion Model
Flowrates: 1 - 1,4262 litres/min.
2 - 2,0795 litres/min.
3 - 2,6765 litres/min.
4 - 3,3011 litres/min.
Experimental Outlet Concentrations +
0,10
0,09
0,08
0,07
0,06
0,05
0,04
0,03
0,02
0,01
0
0
20
40
60
80
100
120
140
160
length (cm)
1
2
3
4
+ 1
+ 2
+ 3
+ 4

FIGURE 9.4

CONCENTRATION PROFILES FOR MONOACETATE

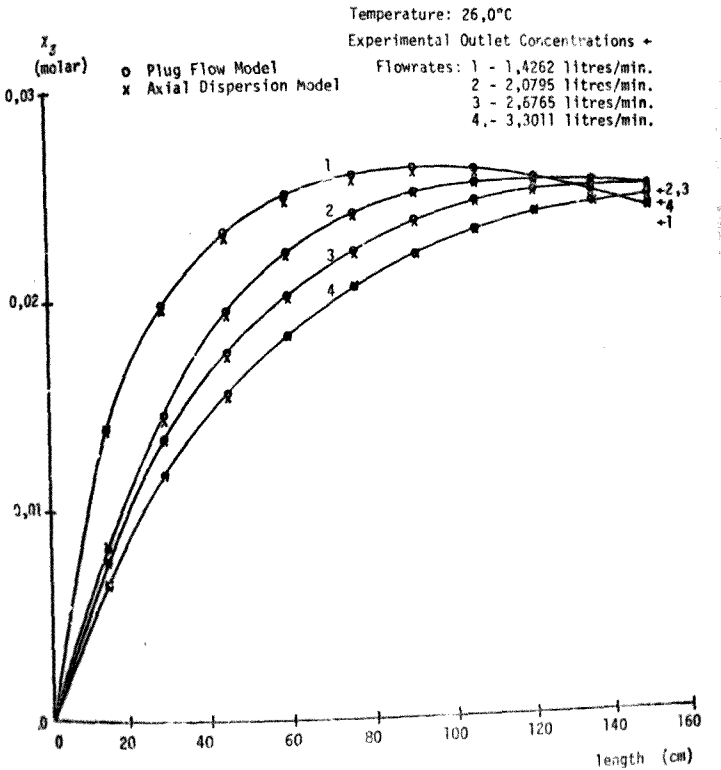

FIGURE 9.5

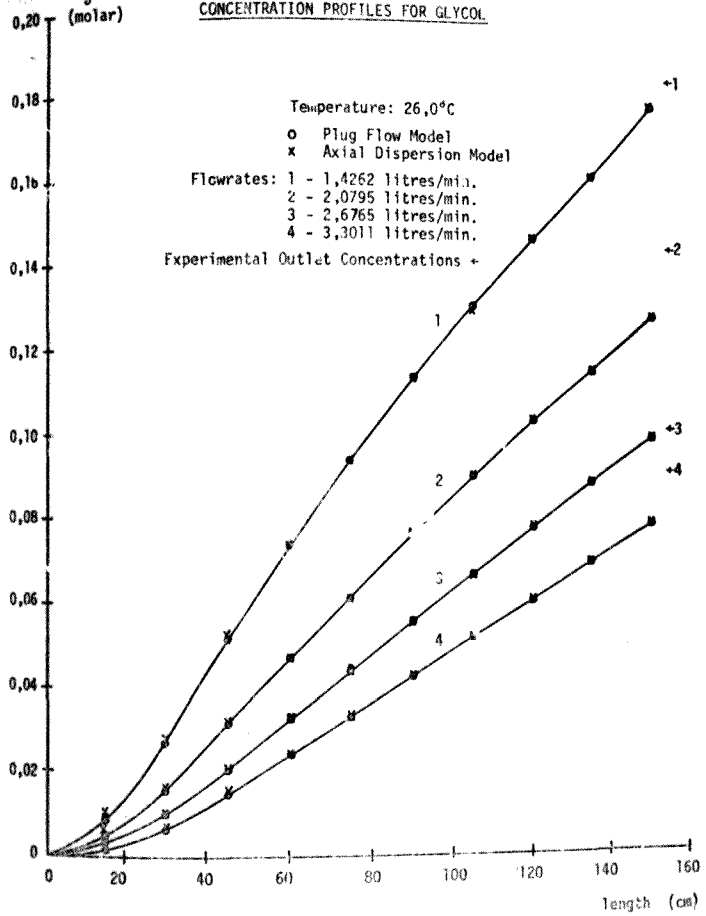
X_5 (molar)
CONCENTRATION PROFILES FOR GLYCOL
Temperature: 26,0°C
o Plug Flow Model
x Axial Dispersion Model
Flowrates: 1 - 1,4262 litres/min.
2 - 2,0795 litres/min.
3 - 2,6765 litres/min.
4 - 3,3011 litres/min.
Experimental Outlet Concentrations +
+1
+2
+3
+4
1
2
3
4
0,20
0,18
0,16
0,14
0,12
0,10
0,08
0,06
0,04
0,02
0
0
20
40
60
80
100
120
140
160
length (cm)

FIGURE 9.6

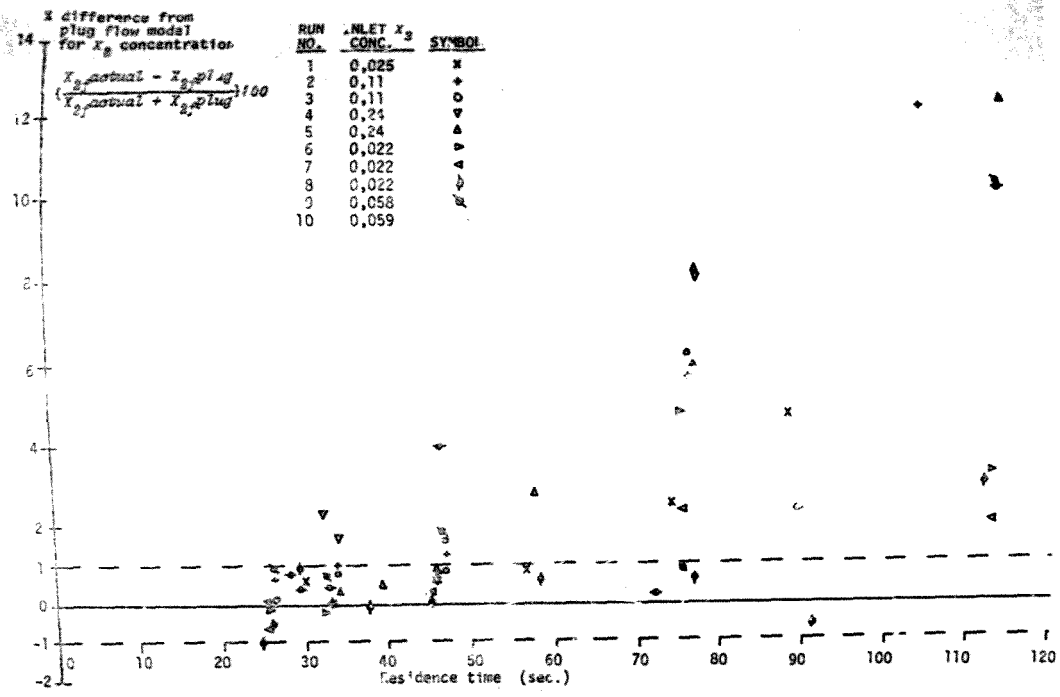

FIGURE 6.7
LATTICE INLET

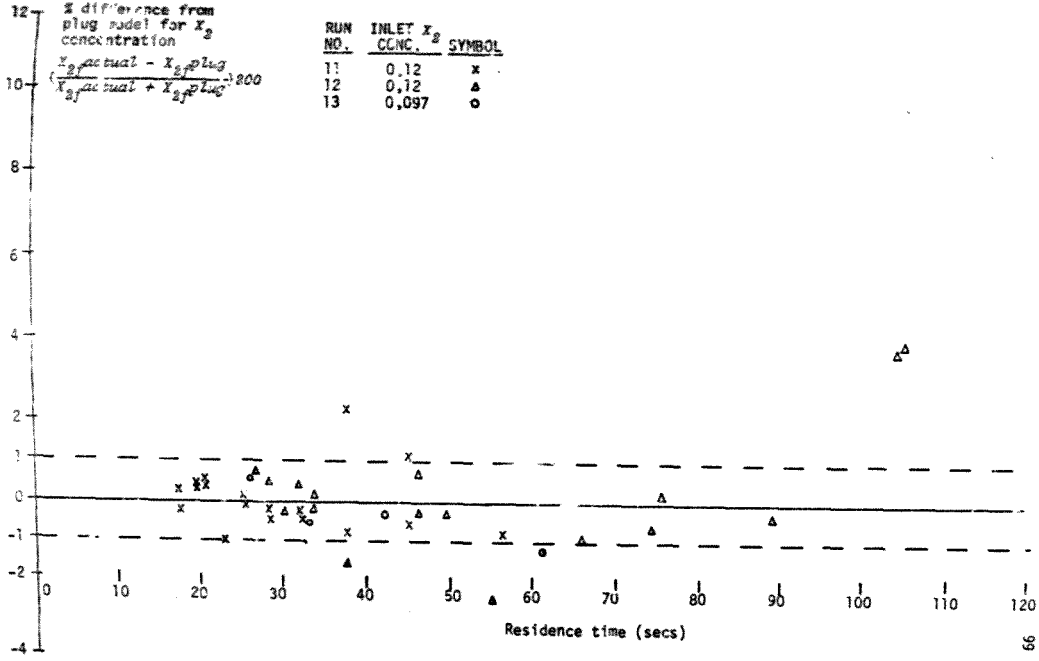

FIGURE 9.8
RING INLET

it is possible to reach a higher maximum concentration of monoacetate in the ideal TFR than in the CSTR. The monoacetate also reacts faster in the ideal TFR, so that as the reactor residence time increases the CSTR concentration eventually becomes greater than the ideal TFR concentration for the same residence time.

This result confirms the assumption made in section 4.2, that the ideal TFR is preferable to the CSTR for carrying out the chosen reactions.

In section 8.5 it was seen that the outlet concentration from the reactor which could be measured most accurately was that of caustic soda. It was consequently decided that this concentration would be used to test the validity of the various models.

Since it was expected that the reactor would obey the plug flow model, this model was tested first by calculating the percentage difference between the actual final caustic concentration and that predicted by the plug flow model, as given in Appendix ix, and plotting this percentage against residence time in the reactor. Figures 9.7 and 9.8 show the results for the T-piece and ring inlets respectively.

It will be seen from the figures that the percentages obtained with the T-piece inlet go up to 12,5%. The standard deviation from 0 is 3,97. The results for the ring inlet have a standard deviation of 1,13 and all points lie below 4%. For residence times from 10-50 seconds, however, the standard deviations become 1,12 and 0,70, for T-piece and ring inlets respectively, indicating that the differences on Figure 9.7 are due to poor mixing in the T-piece. The concentration measurements discussed in Appendix iii confirm this. These measurements also indicated that the mixing in the ring inlet is extremely good. The experimental results with the ring inlet were thus used for all further comparisons with the various models.

From Tables 9.2 and 9.3, it can be seen that outlet concentrations predicted by the segregated flow model were almost identical whether the experimental or calculated residence time distributions were used. This indicates that the variations in residence time distribution functions shown in Figures 6.4-6.16 were not sufficient to affect predicted outlet concentrations.

Also, from Tables 9.2 and 9.3 it can be seen that the segregated flow model predicted almost identical outlet concentrations to the plug flow model. It is thus preferable to use the plug flow model since its solution presents far less difficulties than the solution of the segregated flow model.

All the models used in Figures 9.3-9.6 predict practically identical concentration profiles and final concentrations. The experimental agreement for caustic is excellent, but due to the error growth discussed in section 8.5, the agreement between experiment and theory for the other components is not good. The deviations were all within the limits determined in that section.

These results show that the assumptions made in sections 3.4.2. c and d are correct, and that for the reactor length chosen, the reactor behaves as an ideal TFR. The assumption made in 3.1 that the reactor was isothermal is also correct.

9.3 CONCLUSIONS

For a reaction system of the type:

$$A + B \xrightarrow{k_1} C + D \qquad \text{I}$$

$$C + B \xrightarrow{k_2} D + E \qquad \text{II}$$

where both reactions are second order and irreversible, the following conclusions may be drawn:-

1. For the range of inlet concentrations and operating condi-

tions used in this work , an ideal tubular flow reactor will yield higher outlet concentrations of desired product, C, than an ideal continuous stirred tank reactor.

2. An isothermal temperature policy is the optimum for the ideal tubular flow reactor, with the operating temperature set either at its maximum or minimum value, depending on the activation energies of the two reactions. For the reactions studied, the activation energy of the second reaction was greater than that of the first, which necessitated the operating temperature being set at its minimum value.

3. For a reactor packing particle diameter to overall reactor length ratio of less than 0,01, the ideal tubular flow model and the axial dispersion model yield identical outlet concentrations of each reaction species for reactions in liquid medium. Furthermore the three sets of boundary conditions given in the literature for the axial dispersion model all yield identical results for a reactor with the above dimension ratio.

4. One point sampling methods are adequate for obtaining residence time distribution functions for the reactor, and the distribution functions are not affected by the inlet mixing, or the position of the injection point in the inlet. Unpacking and repacking the column has no effect on the residence time distribution function. The axial diffusion model for pure diffusion is insensitive to the axial mixing coefficient, D_a, but is sensitive to velocity, U.

5. The segregated model, when solved in conjunction with the experimental residence time distribution function, predicts outlet concentrations identical to those predicted by the ideal tubular reactor and axial dispersion models.

6. The type of inlet mixing system chosen has a profound effect on the reactor performance. A ring main type of inlet was found to

give satisfactory mixing.

7. Experimental outlet concentrations agree with those predicted by the ideal tubular reactor, axial dispersion and segregated flow models within the limits set by experimental error. Since the ideal tubular reactor model is the simplest of these, and the easiest to solve, this model should be used when designing packed bed reactors in which the packing particle diameter to overall reactor length ratio is less than 0,01, for reactions in liquid medium.

APPENDIX j

The flowmeters used were Fischer Porter Flowratormeters with a R.4.17 tube 10 inches long, and a BSVT-45 stainless steel float. The tube is calibrated in percentage of full flow, covering a range of 10-100% in steps of 1%. The floats were self cleaning to a degree and in addition fine stainless steel screens were inserted immediately upstream of the rotameters to stop fouling of the floats. Nevertheless it was felt that it would be more accurate to calibrate the rotameters at the end of each run rather than simply to rely on one calibration curve for all runs. In this way, all changes in hydrodynamic properties such as viscosity and density of the fluids run to run would automatically be accounted for.

The rotameters were calibrated at each of the five flow rates used during the run, and also at each of the flowrates used in the residence time distribution experiments, and the procedure was as follows.

The stream to be calibrated was allowed to run to waste through the reactor for times which were double the residence times at that flowrate so that all other solutions were flushed out of the reactor. The temperature was then recorded, and the rotameter was set to the first of the experimental flowrates. An empty measuring cylinder was tared on a Mettler type K4T balance. After the flow had been steady for one minute, the flexible outlet pipe (see Figure 5.4) was switched rapidly to above the measuring cylinder, and a sample of roughly 2 litres was collected. The sample collection was timed using a stopwatch with a 30 second sweep calibrated in 0,1 seconds, and the sample collected was weighed. The flowrate of the stream in kg/minute was then calculated, and the calibration repeated until two flowrates had been obtained at the same rotameter

reading which agreed with each other to better than 99% accuracy. The procedure was repeated at each experimental point in random order.

It was found that the caustic and diacetate rotameters did not give reproducible results at settings below 20 or above 90, these giving minimum and maximum flowrates of 0,38 and 1,65 litres/minute respectively. They were consequently not used outside this range. The acetic acid rotameter range was 15-100, giving flowrates of 0,27 and 1,82 litres/minute.

Originally the calibration curves were plotted for each meter to check that all the points lay on one line, but the fit was always so good that this practice was later abandoned. A typical calibration curve for each rotameter is included on figures A.i.1-3.

Knowing the mass flow rate at each experimental point, the volumetric flowrate could easily be obtained by using the density correlations for each fluid, given in Appendix ii.

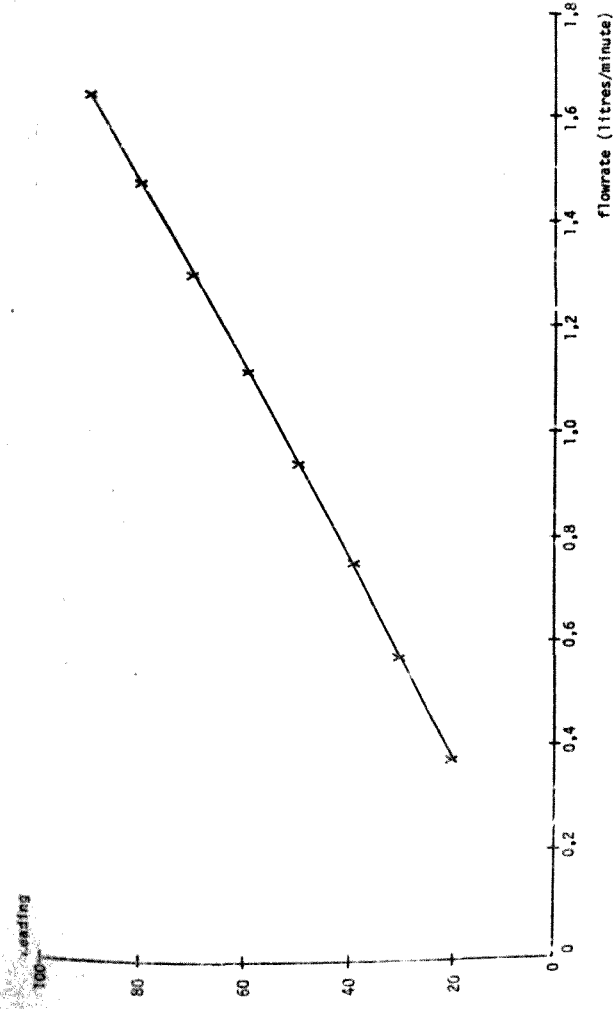

FIGURE A.1.1

STREAM 1 ROTAMETER CALIBRATION

FIGURE A.1

STREAM 2 ROTAMETER CALIBRATION

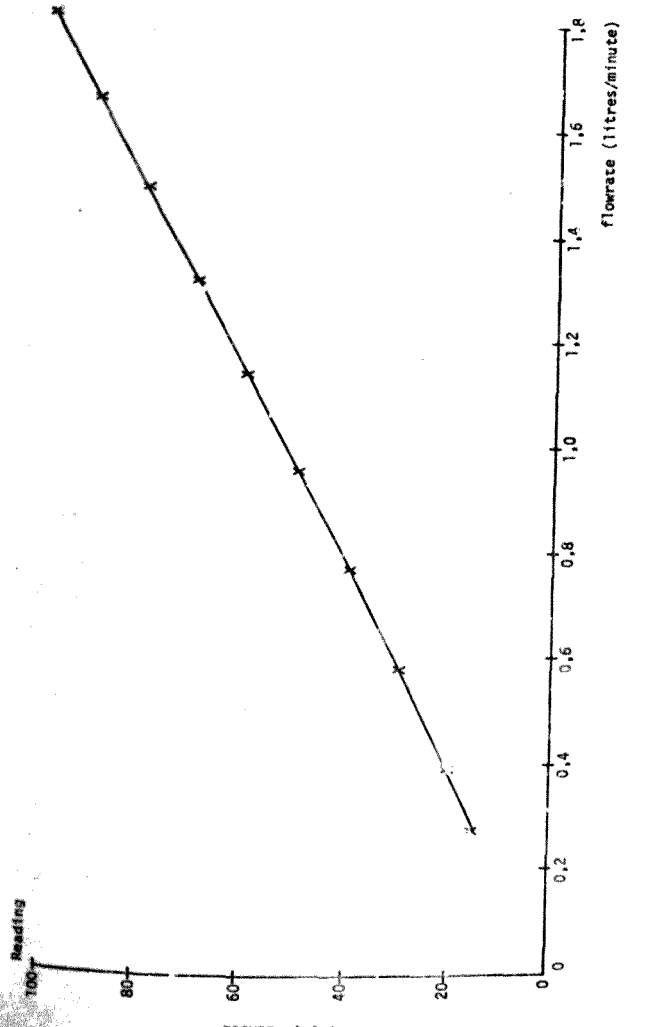

FIGURE A.1.3

STREAM 5 ROTAMETER CALIBRATION

APPENDIX II

Since all rotameter calibrations and all titrations were done by weight, rather than by volume, the densities of all solutions used in this work had to be known.

It was decided that solution densities would be measured in all cases except water, because either tables could not be found for the solutions in question, or the tables did not extend to the dilutions used in this work.

The procedures used were as follows.

If the temperature of the solution was 23°C or lower, the density was simply measured by using an A grade certificated pipette to measure out 20 cm^3 of solution which was weighed on a Mettler H 10 balance. Care was taken to allow the solution to run out for the time stated on the pipette. Three measurements were made and it was found that the greatest variation for any of the density measurements was less than 0,1%.

If the solution temperature was above 23°C, a solid object was weighed in the liquid and then in distilled water at the same temperature, and the loss in weight was used to calculate the density of the solution from the formula:

$$\rho_L = \frac{(w - w_L)\rho_w}{(w - w_w)}$$

ρ_L = density of liquid at temperature t°C

ρ_w = density of water at t°C

w = weight of solid object

w_L = weight of solid object in liquid at t°C

w_w = weight of solid object in water at t°C

The density of water had obviously to be known at any temp-

erature in order to be able to apply this formula, a d tables had to be used to obtain this. Perry (1963) pages 3-40, gives a table of water density versus temperature. In order to obtain intermediate values of density at temperatures not given in the table, the computer was used to fit a polynomial to the points in the table using a least squares fitting technique. The polynomial was then used to print out a table of temperature versus density at 0,1°C intervals between 20 and 30°C. ρ_w could be read off this table at the solution temperature t, and the above formula could then be used to obtain the solution density.

All measured densities were checked with tabulated values wherever possible and the agreement was found to be better than 0,5% in all cases.

APPENDIX iii

Diagrams of the two inlet mixing systems used in this work are given in Figure 5.3. As discussed in 5.2.3, although the T mixer appeared to give ideal mixing when checked visually using dye traces. the experimental reactor results showed that the mixing was far from ideal. In order to test the mixing, therefore, a small conductivity probe was made up which could be inserted through the thermometer boss at the column inlet. The probe consisted of two insulated copper wires, 0,02 inches in diameter, bent to face each other across a 1/16" gap. A diagram of the probe system is given on Figure A.iii.1.

As can be seen from the figures, the probe could be slid across the reactor diameter, so that the concentration at any point on the diameter could be measured. The probe was connected to a conductivity meter whose output could be traced on a 0-1 mV recorder as for the residence time distribution runs. The calibration curve for this detector is given in Figure A.iii.2 and can be seen to be perfectly linear.

Using this probe the inlet radial concentration profiles were measured for both inlets for a range of flow rates with 1,22 gm/litre salt solution flowing in the straight run of the inlets and distilled water flowing in the side branch. Figure A.iii.3 shows the resultant concentration profiles relative to the position of the inlets.

The probe could not be drawn across the whole radius of the tube or the water seal would have been broken, hence the complete profiles could not be obtained, but it is reasonable to assume that these would have continued in a smooth curve.

It can be seen from the figure that with the T-piece, the water forces the salt solution to one side of the reactor and the streams are segregated at the inlet. The ring inlet on the other hand mixes the streams properly and a relatively flat profile results.

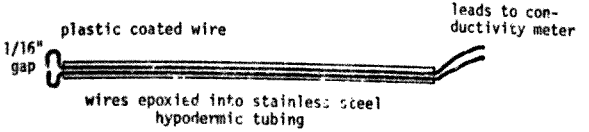

PROBE

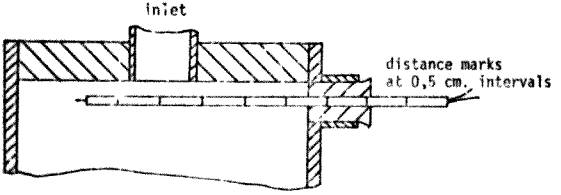

PROBE INSERTED IN REACTOR

FIGURE A.iii.1

CONDUCTIVITY PROBE FOR MEASURING INLET CONCENTRATION PROFILES

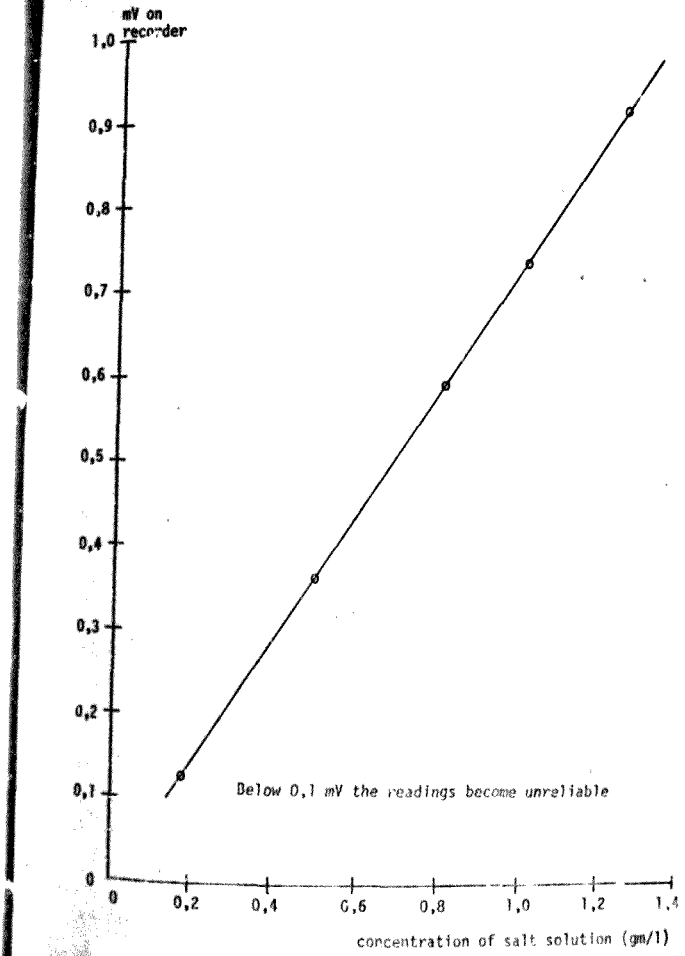

FIGURE A.iii.2

CALIBRATION OF CONDUCTIVITY PROBE

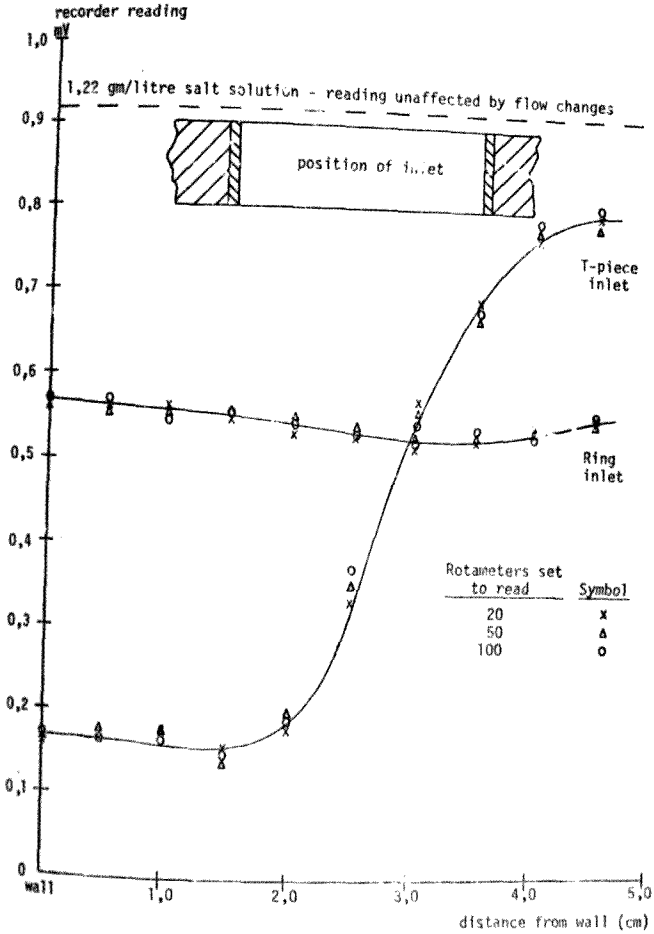

FIGURE A.iii.3

INLET CONCENTRATION PROFILES

APPENDIX iv

It was vital that the reaction should be quenched as soon as the reaction mixture left the reactor. This meant that the mixing of the acetic acid quench stream and the reactor outlet stream had to be rapid enough to neutralise all the caustic soda present before it could react further with the diacetate or monoacetate. Once the quench system had been built, therefore, it was necessary to test it to check that the saponification reaction was quenched with sufficient speed.

1. EXPERIMENTAL PROCEDURE

Caustic soda was allowed to flow through the reactor in the normal way, but an extra flow line for the diacetate was constructed which utilised the diacetate rotameter but which terminated directly over the reactor outlet pipe (see Figure 5.4). The acetic acid quench stream entered the reactor in the normal way. This arrangement ensured that the caustic soda leaving the reactor would mix with the diacetate before coming into contact with the acetic acid.

Stock solutions were made up and sampled in the normal way, and their temperatures were recorded. With the caustic soda and diacetate flows set approximately at each of the values used during the main runs, the acetic acid flowrate was then adjusted to give the desired pH in the outlet quench beaker.

The flowmeter readings on the caustic soda and acetic acid lines were recorded, and at the end of the run each of these flowmeters was calibrated using the procedure in Appendix i. It was not necessary to record the diacetate flow rate, provided that this was set equal to the caustic flowrate at each point, because this stream was merely provided to compete with the acetic acid in the quench

vessel.

It was decided that the diacetate stock concentration would be set to half that of the caustic soda stock concentration. The diacetate and caustic soda thus entered the quench vessel in the ratios in which they would normally enter the reactor.

2. RESULTS AND CALCULATIONS

Two sets of runs were done, one at high, and one at low, inlet concentration. The stock concentrations used were as follows:-

TABLE A.iv.1

	Run 1	Run 2
NaOH	0,1138 M	0,4765 M
Diacetate (HAc free)	≈0,05 M	≈0,2 M
HAc	0,1070 M	0,4232 M

At the run temperature,

density of NaOH, ρ_2	1,0026 g/cm^3	1,0183 g/cm^3
density of HAc, ρ_5	0,9985 g/cm^3	1,0012 g/cm^3

During the run, the flows of diacetate and caustic were set equal so that the concentrations of caustic entering the outlet quench vessel were equal to half the stock concentrations.

The following flowrates were obtained from the two runs:-

TABLE A.iv.2

RUN 1

NaOH flowmeter setting	NaOH flowrate G_2 (kg/min)	HAc flowrate G_5 (kg/min)
20,0	0,3767	0,3997
30,0	0,5813	0,6139
50,0	0,9564	1,0097
70,2	1,3098	1,3947
90,5	1,6648	1,7645

RUN 2

20	0,3943	0,4350
29,7	0,5925	0,6591
49,7	0,9731	1,0709
70,1	1,3364	1,4735
86,1	1,6152	1,7909

It will be noted that the above rotameter settings correspond approximately to the 20, 30, 50, 70 and 90 used in the main runs.

Now, if the outlet quench were perfect, then the HAc would be exactly equivalent to the NaOH in the outlet.

Hence for Run 1, by mole balance:-

$$\frac{(G_2)(0,1138)}{1,0026} = \frac{(G_5)(0,1070)}{0,9985}$$

For perfect quenching, therefore,

$$\frac{G_2}{G_5} = \frac{(0,1070)(1,0026)}{(0,1138)(0,9985)} = 0,9441$$

Similarly for Run 2,

$$\frac{G_2}{G_5} = \frac{(0,4232)(1,0183)}{(0,4768)(1,0013)} = 0,9033$$

The actual ratios of $\frac{G_2}{G_5}$ obtained, and the percentage differences from the above values are given in Table A.iv.3.

TABLE A.iv.3

RUN 1		RUN 2	
Ratio $\frac{G_2}{G_5}$	% difference from ideal ratio	Ratio $\frac{G_2}{G_5}$	% difference from ideal ratio
0,9425	-0,17	0,9064	+0,34
0,9467	+0,28	0,8990	-0,48
0,9472	+0,33	0,9087	+0,60
0,9391	-0,53	0,9070	+0,41
0,9435	-0,06	0,9019	-0,16

Since pure diacetate was fed directly to the outlet quench vessel from the stock tank, the concentration of diacetate was considerably higher in the quench vessel during these runs than in the main runs where the diacetate was partially converted in the reactor first. The concentrations above thus represent the worst possible operating conditions for the outlet quench system.

3. DISCUSSION

In all cases above, the experimental ratio is within 99% of the ratio for perfect quenching. It may thus be assumed that the quench system was operating satisfactorily for these runs. As expected, changing the concentrations of all streams entering the quench vessel proportionately does not affect the degree of quenching since this depends only on the mixing in the vessel and the relative rates of reaction of the components. It may thus be assumed that the outlet quench system operated satisfactorily for the